Biometric Systems
Lesson 10: Iris recognition

Maria De Marsico
demarsico@di.uniroma1.it

SAPIENZA
UNIVERSITÀ DI ROMA

Dipartimento di Informatica

Credits

- This lesson contains some material from a lesson by Prof. Michele Nappi and Prof. Daniel Riccio of University of Naples – BIPLAB at University of Salerno

Iris

- The iris is a muscle membrane of the eye, of variable color, with both shape and function of a diaphragm
- It is pigmented, located posterior to the cornea and in front of the lens, and is perforated by pupil.
- It consists of a flat layer of muscle fibers which circularly surround the pupil, a thin layer of smooth muscle fibers by means of which the pupil is dilated (thereby regulating the amount of light that enters the eye) and posteriorly by two layers of epithelial pigmented cells
- Iris colour, “regular” texture (mostly by furrows) and “irregular” patterns (e.g., freckles and crypts) provide a very high level of discrimination, which is comparable to fingerprints

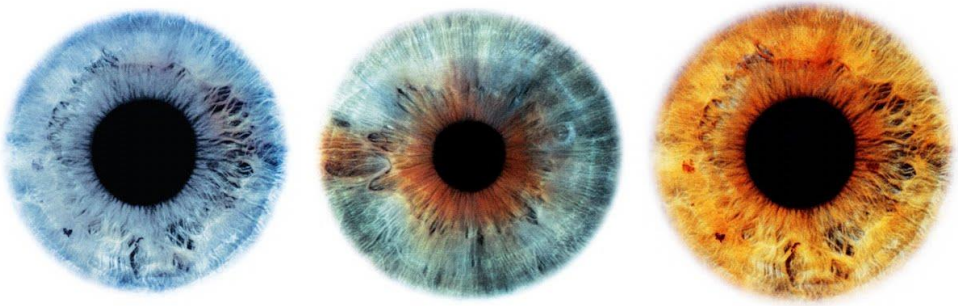

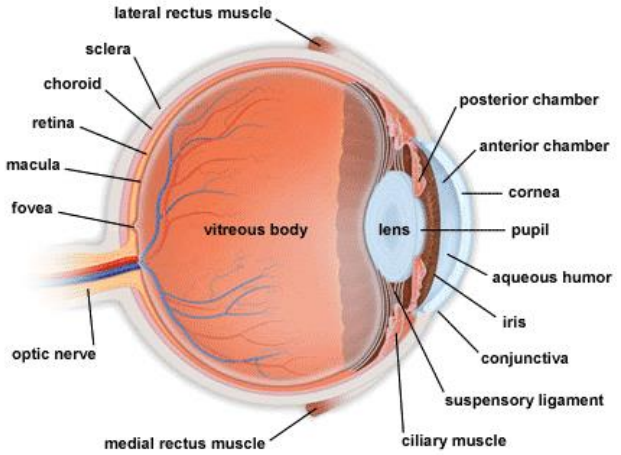

The Afghan Monna Lisa

- 1984: in a refugee camp in Pakistan
- 2002: (18 years later) in Afghanistan

photographed twice by McCurry from National Geographic.

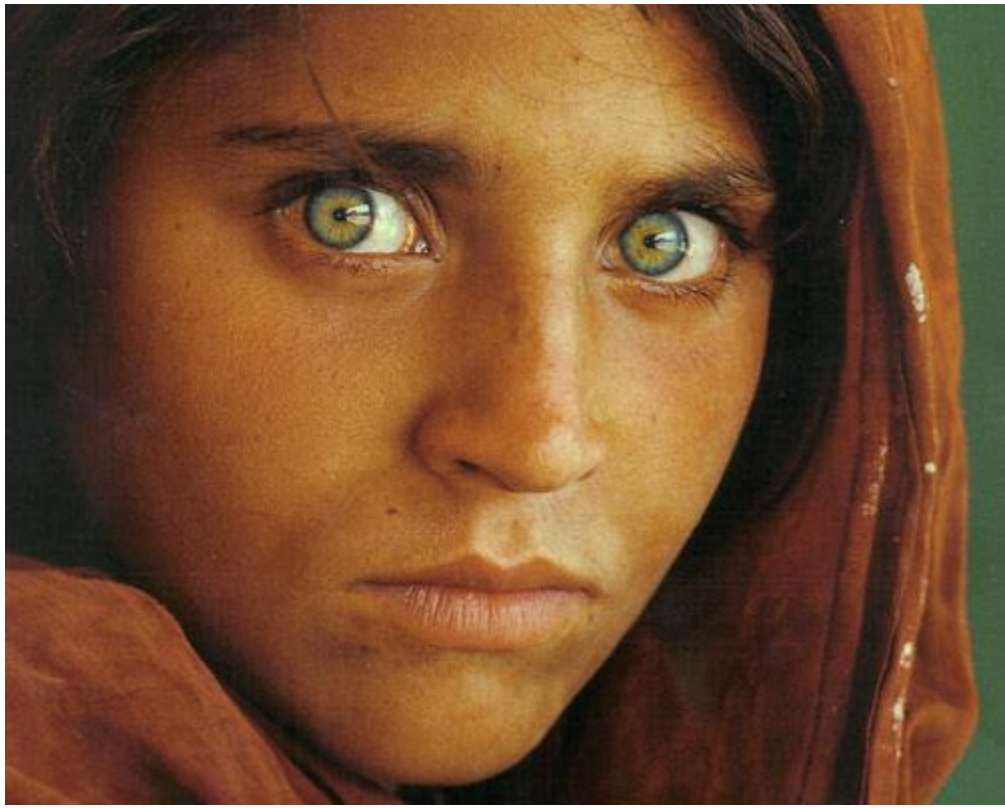

The Afghan Monna Lisa

- 1984: in a refugee camp in Pakistan
- 2002: (18 years later) in Afghanistan

photographed twice by McCurry from National Geographic.

The Afghan Monna Lisa

- 1984: in a refugee camp in Pakistan
- 2002: (18 years later) in Afghanistan

photographed twice by McCurry from National Geographic.

The Afghan Monna Lisa: Sharbat Gula

- 1984: in a refugee camp in Pakistan
- 2002: (18 years later) in Afghanistan

photographed twice by McCurry from National Geographic.

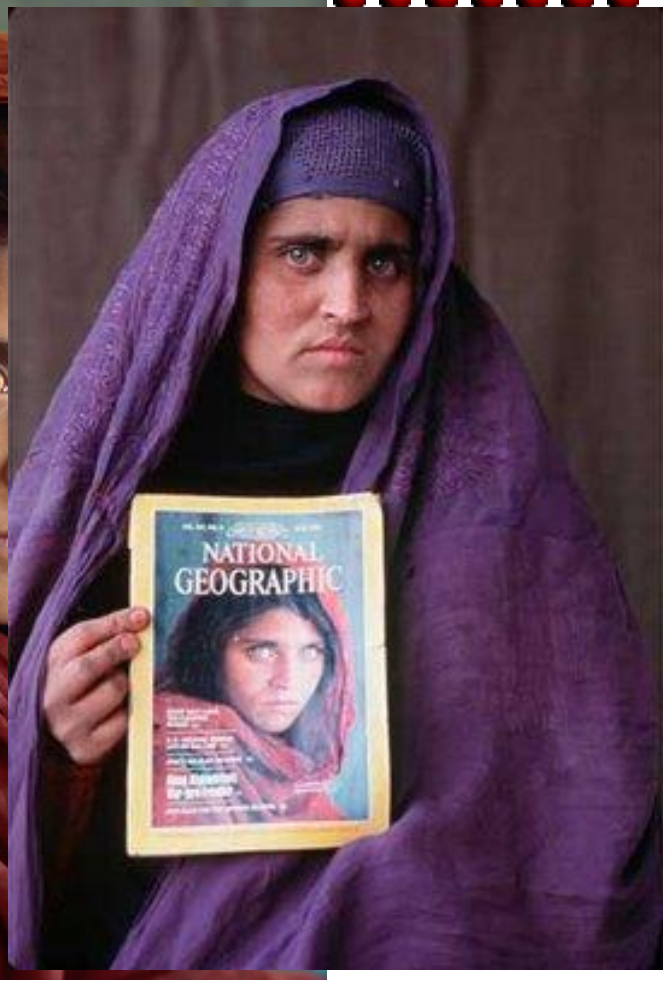

National Geographic Society

Biometric Overview

Biometric characteristic	*genotypic**	*randotypic**	*behavioral***
Fingerprint (only minutia)	o	ooo	o
Signature (dynamic)	oo	o	ooo
Facial geometry	ooo	o	o
Iris pattern	o	ooo	o
Retina (Vein structure)	o	ooo	o
Hand geometry	ooo	o	o
Finger geometry	ooo	o	o
Vein structure of the hand	o	ooo	o
Ear form	ooo	o	o
Voice (Tone)	ooo	o	oo
DNA	ooo	o	o
Odor	ooo	o	o
Keyboard Strokes	o	o	ooo

Biometric Trait	*Permanence over time*
Fingerprint (Minutia)	oooooo
Signature(dynamic)	oooo
Facial structure	ooooo
Iris pattern	ooooooooo
Retina	oooooooo
Hand geometry	ooooooo
Finger geometry	ooooooo
Vein structure of the back of the hand	oooooo
Ear form	oooooo
Voice (Tone)	ooo
DNA	ooooooooo
Odor	oooooo ?
Keyboard strokes	oooo

Biometric Overview

Template Size

Biometric	Approx Template Size
Voice	70k – 80k
Face	84 bytes – 2k
Signature	500 bytes – 1000 bytes
Fingerprint	256 bytes – 1.2k
Hand Geometry	9 bytes
Iris	256 bytes – 512 bytes
Retina	96 bytes

Iris Recognition

Pros

- Iris is visible yet well protected
- It is a time invariant (after about 2 years age) and extremely distinguishing trait (right different from left and even twins have different irises)
- Its image can be acquired without direct contact
- Acquisition: near infrared and visible wavelenghts

Cons

- Iris' surface is very limited: only about 3.64 cm2
- A "good" acquisition requires a distance of less than one meter to guarantee a sufficient resolution, depending on the input device.

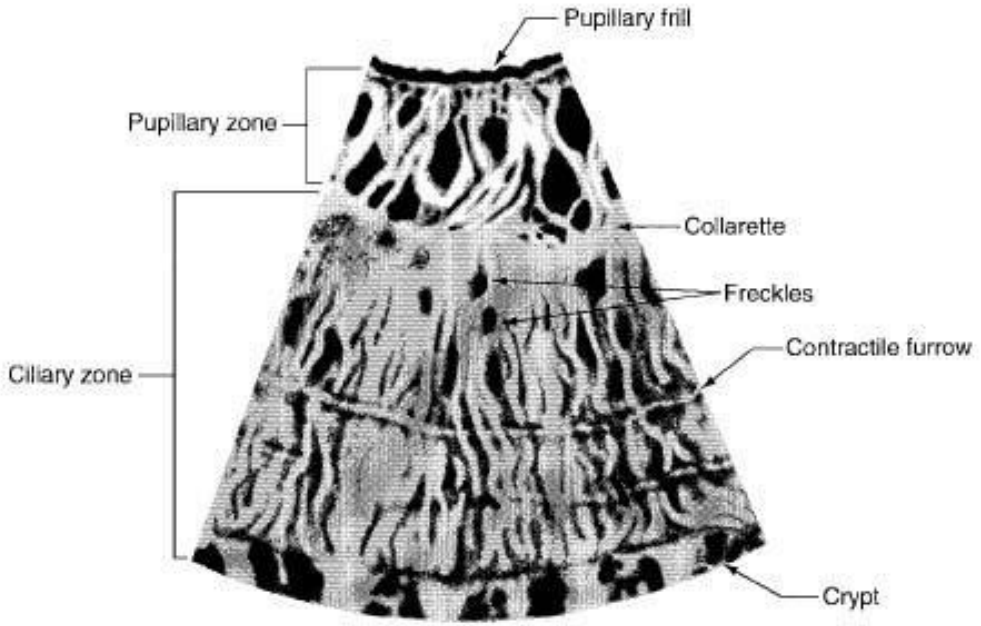

Iris recognition

Possible problems

- Small size (11mm)
- High resolution (200 pixels)
- Limited depth of field
- Need to align with optical axis
- Need to consider gaze direction
- Specular reflections
- Possible presence of glasses
- Possible presence of contact lenses

BioEnable Single Eye iris Scanner called BioEnable Iris One

Iris recognition

Possible solutions

- CCD with high resolution
- Optical system designed to improve the depth of field (DOF: Depth of Field)
- Mirror to support the user in optically aligning the eye
- Auto-focus system according to the adaptive distance between the eye and the camera

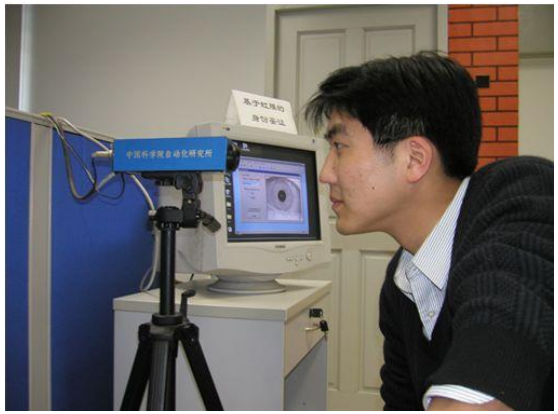

- Using a distance sensor or estimate of the distance based on the content of the captured image
- Audio or visual feedback to the user
- Dual-eye iris camera
- Pan / tilt devices to handle different heights and poses
- Detection and tracking of the face to guide the acquisition of the iris
- Infrared or near-infrared acquisition

Capture modalities

Visible light

- Melanin absorbs visible light
- The layers that make up the iris are well visible
- The image contains noisy information on texture

Infrared light

- The melanin reflects most of the infrared light
- The texture is more visible
- Best suited in biometric systems based on iris recognition but requires special equipment

Capture modalities

- In the visible band of light, the iris reveals a very rich, random, interwoven texture (the “trabecular meshwork”)

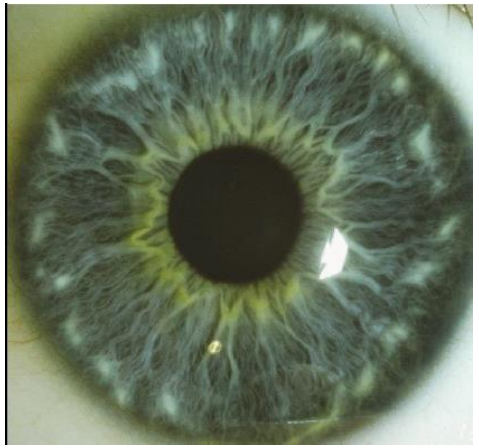

- In infrared illumination even dark brown eyes show a rich texture

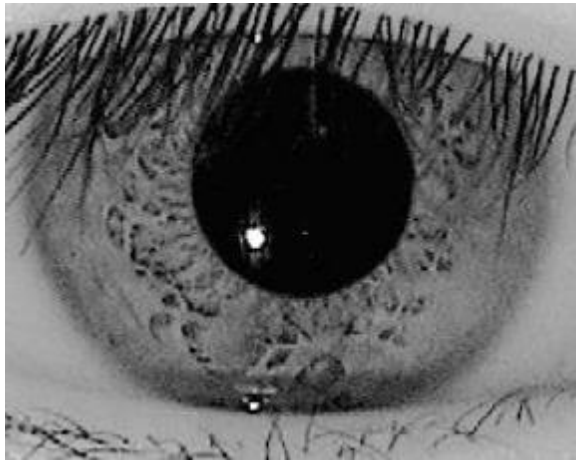

Processing phases

- The presence of a number of noisy elements requires a good pre-processing/segmentation

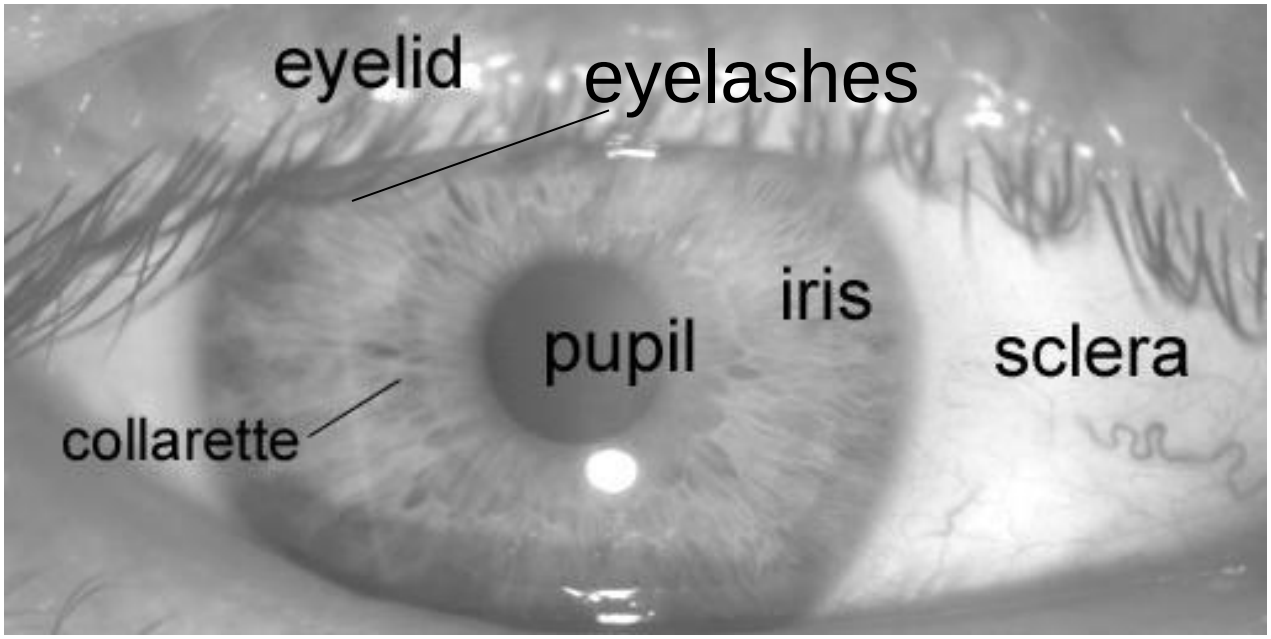

Processing phases

- Segmentation
- Normalization
- Coding
- Matching

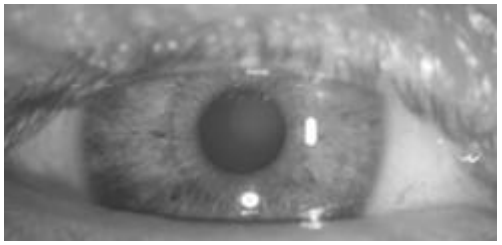
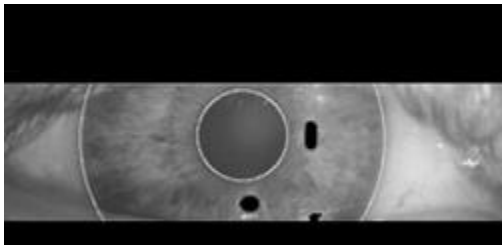
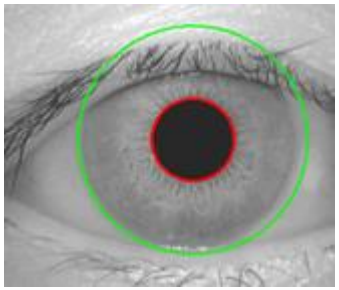

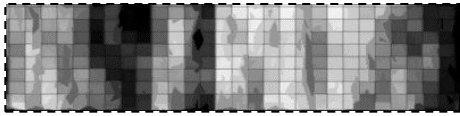
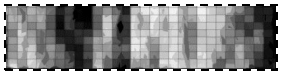
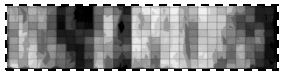

δ

The first and most famous: Daugman

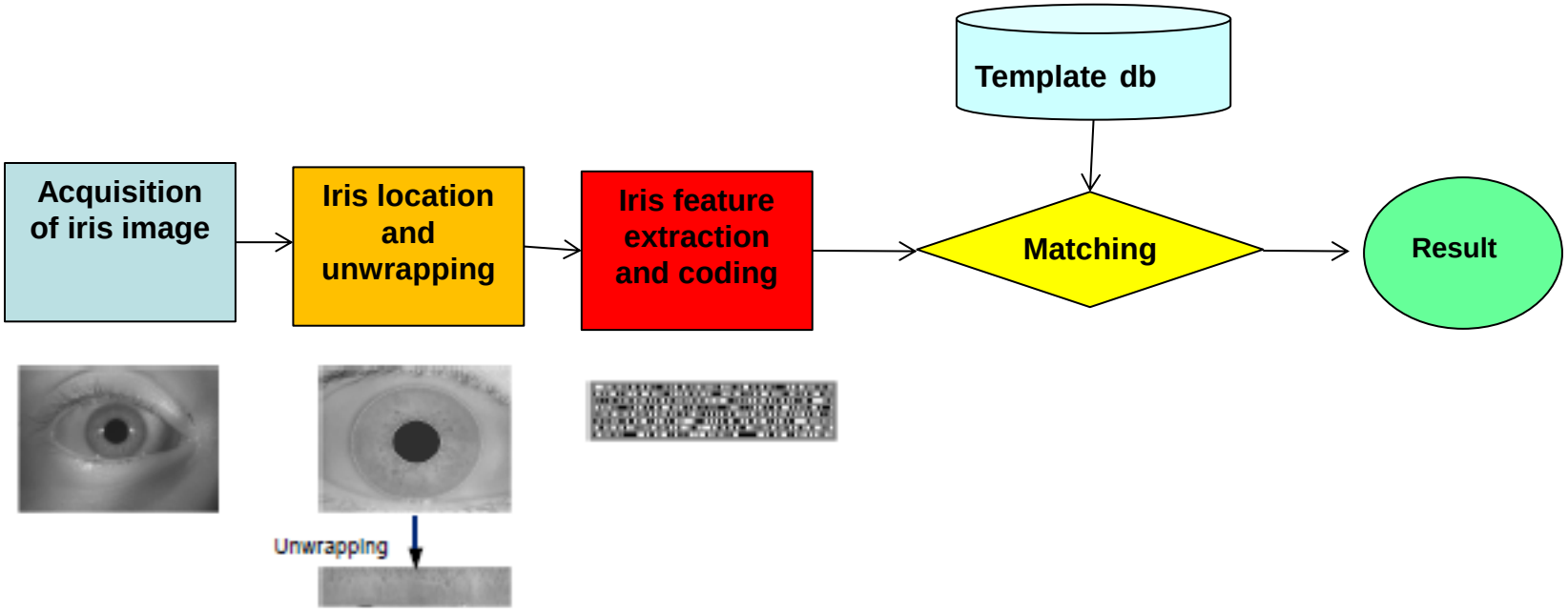

Daugman: iris location

- The approach uses a kind of circular edge detector to localize both the pupil and the iris (integro-differential operator)
- The operator exploits the convolution of the image with a Gaussian smoothing function with center r_0 and standard deviation σ

$$G_\sigma(r) = \left(1/\sqrt{2\pi}\sigma\right)\exp\left[-(r-r_0)^2/2\sigma^2\right]$$

- The operator looks for a circular path along which pixel variation is maximized, by varying the center *r* and radius *(x0, y0)* of a candidate circular contour

$$\max_{(r,x_0,y_0)}\left|G_\sigma(r) * \frac{\partial}{\partial r}\oint_{r,x_0,y_0}\frac{I(x,y)}{2\pi r}ds\right|$$

* Is the convolution operator

- When the candidate circle has the same radius and center of the iris, the operator should provide a peak

Daugman: iris location

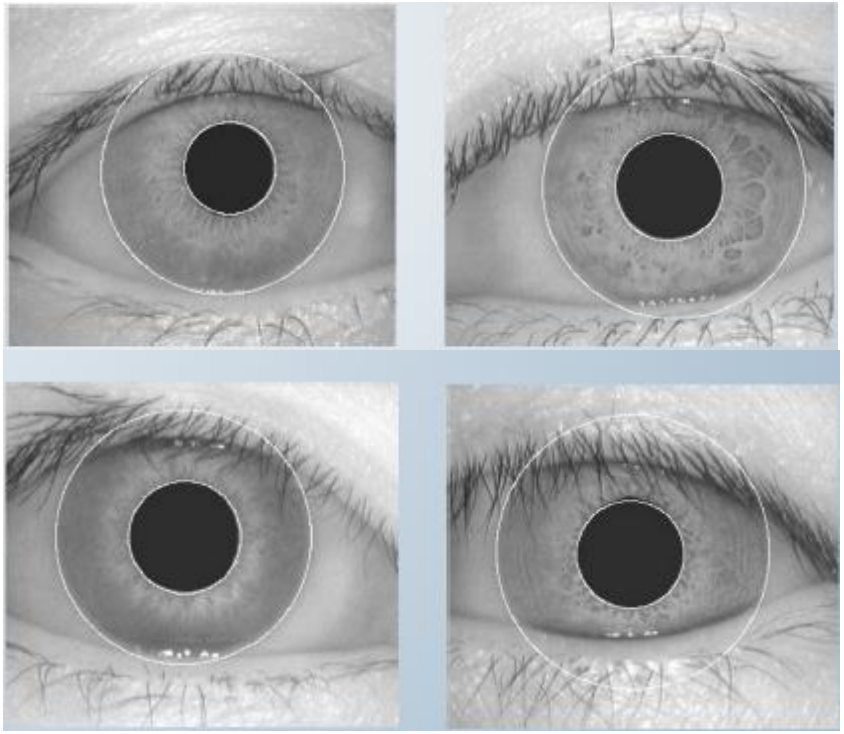

Daugman: eyelids location

- Similar procedure, but instead of looking for circular paths the operator looks for archs, which are approximated by splines

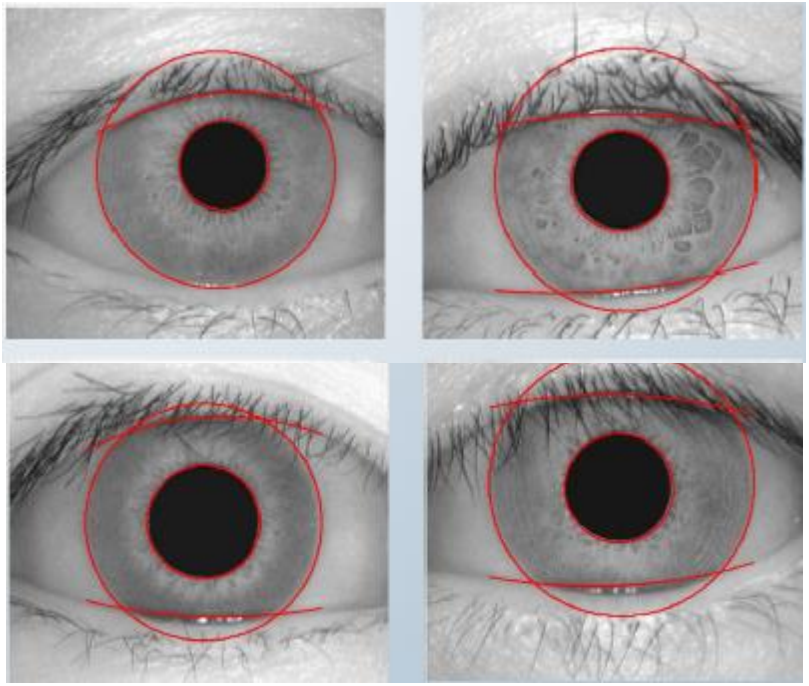

General: iris segmentation

- We obtain a mask so that only iris pixels are further processed

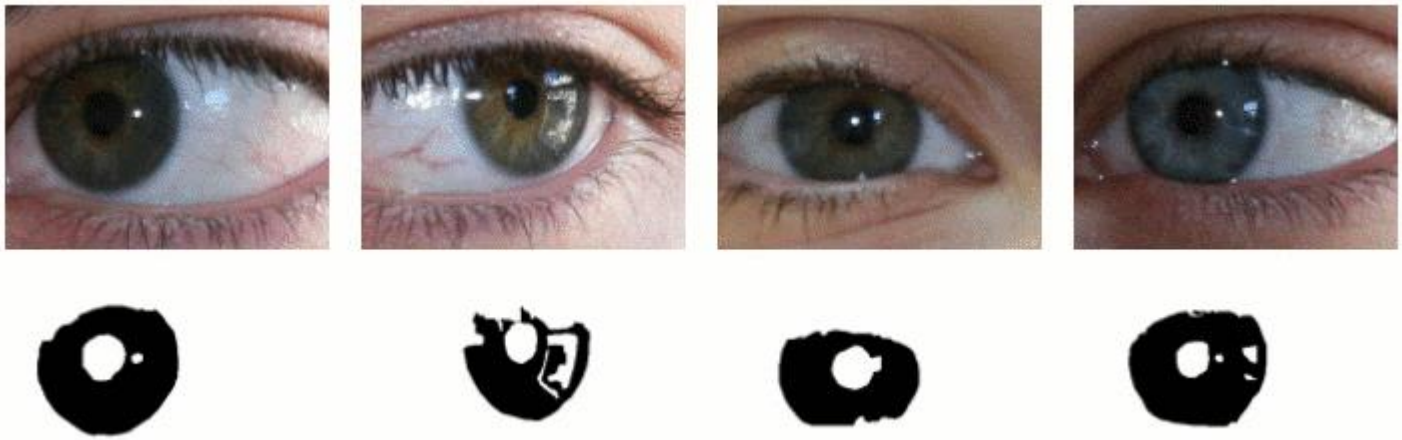

From http://nice2.di.ubi.pt/

Daugman: iris unwrapping

- Polar coordinate make iris processing simpler (circular bands become horizontal stripes, the overall iris annulus becomes a rectangle)
- Determining the right centre for the polar coordinates is of paramount importante but …
- … pupil and iris are not perfectly concentric and …
- … size of the pupil can change due to illumination or pathological conditions (drunk or drugs)
- Gaze direction can change the relative positions of sclera, iris and pupil
- It is necessary to devise a normalization procedure: Rubber Sheet Model

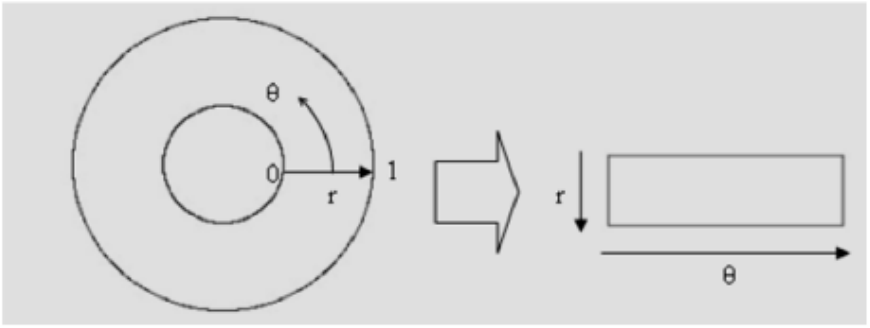

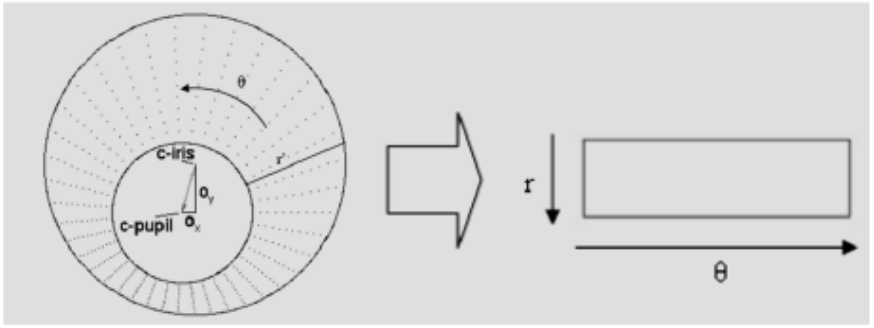

Rubber Sheet Model

- The model maps each iris point onto polar coordinates (r, θ), with $r \in [0,1]$ and $\theta \in [0, 2\pi]$.
- The model compensates for pupil dilation and size variations by producing and invariant representation.
- The model does not compensate for rotations. However, during matching, in polar coordinates, this is done by translating the obtained iris template until alignement.
- The transformation works as follows:

$$I\big(x(r,\theta), y(r,\theta)\big) \rightarrow I(r,\theta)$$
$$x(r,\theta) = (1-r)\cdot x_p(\theta) + r \cdot x_l(\theta)$$
$$y(r,\theta) = (1-r)\cdot y_p(\theta) + r \cdot y_l(\theta)$$

- $(x(r,\theta), y(r,\theta))$ are defined as a linear combination of a set of points $(x_p(\theta), y_p(\theta))$ and of a set of points $(x_l(\theta), y_l(\theta))$, which are respectively the coordinates of the pupil contour and and those of the external iris contour (limbus) which delimits the sclera.

Daugman: feature extraction

- Feature are extracted by applying Gabor filters to the $I(r,\theta)$ image in polar coordinates

$$G(r,\theta) = e^{-i\omega(\theta-\theta_0)} e^{-(r-r_0)^2/\alpha^2} e^{-i(\theta-\theta_0)^2/\beta^2}$$

(r,θ) is the position, α and β are the filter dimensions and ω its frequency

$$h_{\{Re,Im\}} = \operatorname*{sgn}_{\{Re,Im\}} \int\int I(\rho,\phi) e^{-i\omega(\theta_0-\phi)} e^{-(r_0-\rho)^2/\alpha^2} e^{-(\theta_0-\phi)^2/\beta^2} \rho \; d\rho \, d\phi$$

Complex pixel

- For each element with coordinates (r, θ) in the image I(ρ,φ), the method computes a pair of bits as follows

$$h_{Re} = 1 \qquad \mathrm{Re}\left(\int\int I(\rho,\phi) e^{-i\omega(\theta_0-\phi)} e^{-(r_0-\rho)^2/\alpha^2} e^{-(\theta_0-\phi)^2/\beta^2} \rho \; d\rho \, d\phi \right) \geq 0$$

$$h_{Re} = 0 \qquad \mathrm{Re}\left(\int\int I(\rho,\phi) e^{-i\omega(\theta_0-\phi)} e^{-(r_0-\rho)^2/\alpha^2} e^{-(\theta_0-\phi)^2/\beta^2} \rho \; d\rho \, d\phi \right) < 0$$

$$h_{Im} = 1 \qquad \mathrm{Im}\left(\int\int I(\rho,\phi) e^{-i\omega(\theta_0-\phi)} e^{-(r_0-\rho)^2/\alpha^2} e^{-(\theta_0-\phi)^2/\beta^2} \rho \; d\rho \, d\phi \right) \geq 0$$

$$h_{Im} = 0 \qquad \mathrm{Im}\left(\int\int I(\rho,\phi) e^{-i\omega(\theta_0-\phi)} e^{-(r_0-\rho)^2/\alpha^2} e^{-(\theta_0-\phi)^2/\beta^2} \rho \; d\rho \, d\phi \right) < 0$$

$r_0, \theta_0, \alpha, \beta$ e ω are discretized to obtain a 256 byte code, plus a mask of the same size to identify valid iris elements

Iris code

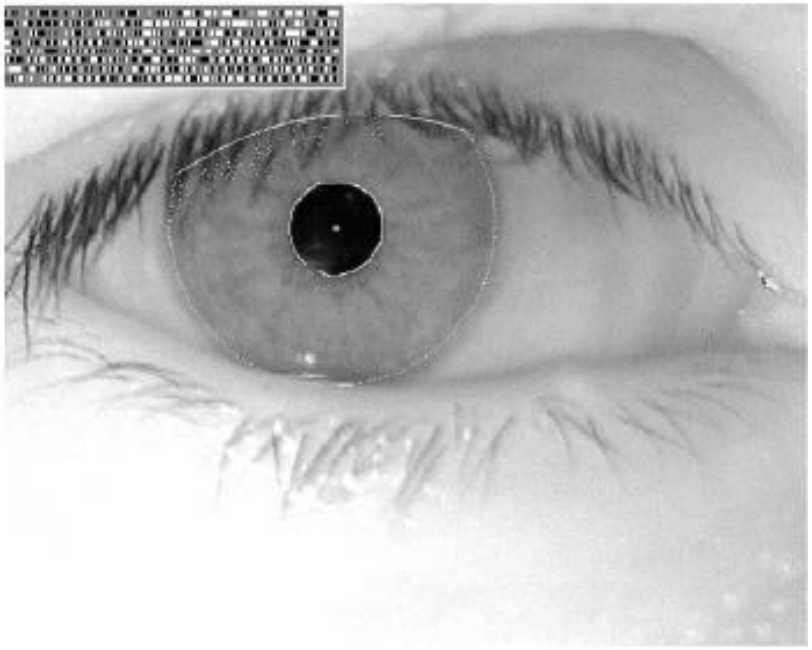

Matching: Hamming distance

$$HD = \frac{1}{N}\sum_{j=1}^{N} A_j \otimes B_j$$

Matching: Hamming distance with mask

$$\mathrm{HD} = \frac{\|(codeA \otimes codeB) \cap maskA \cap maskB\|}{\|maskA \cap maskB\|}$$

NICE: Noisy Iris Challenge Evaluation

- Iris biometric evaluation initiative that received worldwide participations
- Two phases:
  - **NICE.I** evaluated iris segmentation and noise detection techniques
  - **NICE.II** evaluated encoding and matching strategies for biometric signatures.

NICE Dataset

- The **UBIRIS** databases (http://iris.di.ubi.pt/)were developed by the **SOCIA Lab**. (Soft Computing and Image Analysis Group) of the University of Beira Interior (Portugal) (http://socia-lab.di.ubi.pt/).

- They contain visible wavelength iris images captured in heterogeneous lighting conditions, which leaded to the appearance of highly degraded images.

NICE Dataset

- The imaging framework used in the acquisition of the UBIRIS data set was installed in a lounge under both natural and artificial lighting sources.

- A large majority of the volunteers were:
  - Latin Caucasian (approximately 90%)
  - Black (8%)
  - Asian (2%).

NICE Dataset

- Several marks were placed on the floor between three and ten meters away from the acquisition device
- Two distinct acquisition sessions were performed each lasting two weeks and separated by an interval of one week.
- From the first to the second session, both the location and orientation of the acquisition device and artificial light sources were changed.
- Approximately 60% of the volunteers participated in both imaging sessions, whereas 40% participated exclusively in one or the other.

NICE Dataset

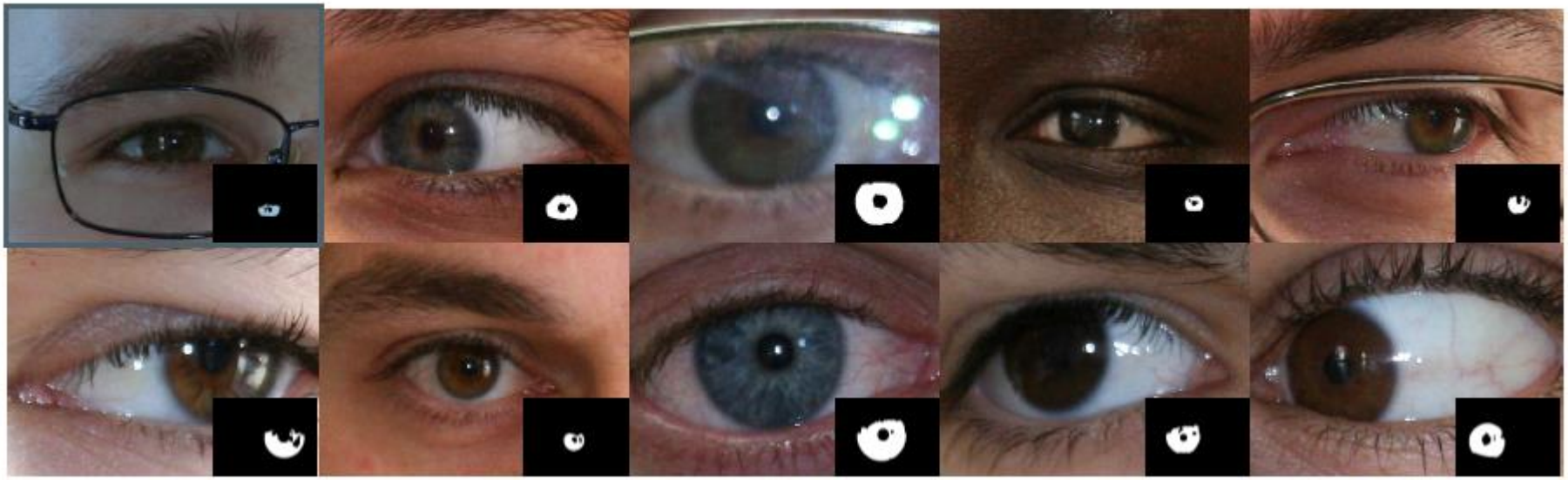

NICE I: iris segmentation

NICE I Committees

Contest Chairs:

- **Hugo Proença**, Department of Computer Science, SOCIA Lab., IT-Networks and Multimedia Group, University of Beira Interior.
- **Luís A. Alexandre**, Department of Computer Science, SOCIA Lab., IT-Networks and Multimedia Group, University of Beira Interior.

Organizing Committee:

- **David Carvalho,** Department of Computer Science, University of Beira Interior.
- **João Oliveira,** Department of Computer Science, SOCIA Lab., University of Beira Interior.
- **Ricardo Santos,** Department of Computer Science, SOCIA Lab., University of Beira Interior.
- **Sílvio Filipe,** Department of Computer Science, SOCIA Lab., University of Beira Interior.

NICE I: iris segmentation

- NICE I received a total of 97 participants from over 22 countries.
- **September 30th, 2008**: The deadline for the final submission of the participations
- **October 15th, 2008:** The classification of the best participants is available.

NICE I: iris segmentation

The Protocol

- The submitted application executable could be written in any programming language and had to run in standalone mode, in one of the operating systems:”Windows XP, Service Pack 2” or ”Fedora Core 6”.

- There was no internet access during the NICE.I evaluation. Thus, the application executable needed to be installed and executed without access to the internet.

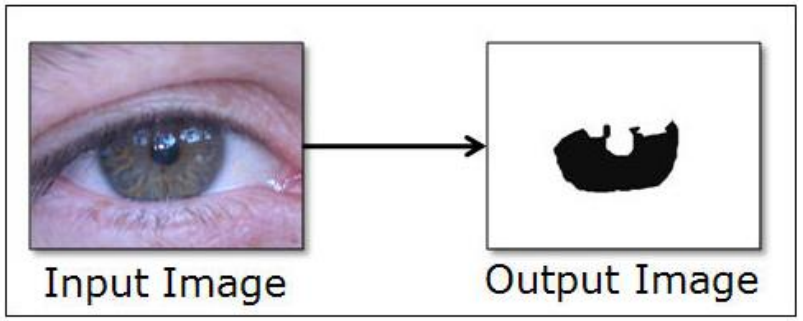

NICE I: iris segmentation

Evaluation

1. Let **Alg** denote the submitted executable, which performs the segmentation of the noise free regions of the iris.
2. Let **$I=\{I_1,\ldots,I_n\}$** be the data set containing the input close-up iris images.
3. Let **$O=\{O_1,\ldots,O_n\}$** be the output images corresponding to the above described inputs, such that **$Alg(I_i)=O_i$**.
4. Let **$C=\{C_1,\ldots,C_n\}$** be the manually classified binary iris images, provided by the NICE.I Organizing Committee. **It was to be assumed that** each **C_i** contains the perfect iris segmentation and noise detection result (**ground truth**) for the input image **I_i**.
5. All the images of **I**, **O** and **C** had the same dimensions: **c** columns and **r** rows.
6. Two measures of evaluation were used:
   - The **classification error rate (E^1)**
   - **The type-I and type-II error rate (E^2)**

NICE I: iris segmentation

Evaluation

- The **classification error rate (E^1)** of the **Alg** participant on the input image I_i **(E_i^1)** is given by the proportion of correspondent disagreeing pixels (through the logical exclusive-or operator) over all the image:

$$E_i = \frac{1}{c \times r} \sum_{c'} \sum_{r'} O(c', r') \otimes C(c', r') \qquad (1)$$

where **O(c',r')** and **C(c',r')** are, respectively, pixels of the output and class images.

- The classification error rate **(E^1)** of the **Alg** participant is given by the average of the errors on the input images E_i:

$$E = \frac{1}{n} \sum_{i} E_i \qquad (2)$$

- The value of **(E^1)** ranges in the [0, 1] interval and **was the main measure of evaluation and classification of the NICE.I participants**. In this context, "1" and "0" were respectively the worst and optimal values.

NICE I: iris segmentation

Evaluation

- The second error measure aimed at compensating the disproportion between the a-priori probabilities of “iris” and “non-iris pixels in the images. The **type-I and type-II error rate (E^2)** of the image E_i is given by the average between the false-positives (FPR) and false-negatives (FNR) rates:

$$\mathbf{E_i = 0.5 * FPR + 0.5\ FNR}$$

- Similarly to the E^1 error rate, the final E^2 error rate was given by the average of the errors (E_i) on the input images.

NICE I: iris segmentation

- The best 8 participants, that achieved the lowest test error rates were invited to publish their approach in a Special Issue on the Segmentation of Visible Wavelength Iris Images Captured At-a-distance and On-the-move Image, *Elsevier Image and Vision Computing 28 (2010)*

Ranking	Username	Affiliation	Country	Error (E1)
1	CASIA	National Laboratory of Pattern Recognition, Institute of Automation, Chinese Academy of Sciences	China	0,0131
2	DMCS	Department of Microelectronics and Computer Science, Technical University of Lodz	Poland	0,0162
3	Palmeida	Department of Computer Science, University of Beira Interior	Portugal	0,0180
4	PeihuaLi	College of Computer Science and Technology, Heilongjiang University	China	0,0224
5	Kang Ryoung Park	Dept. of Electronics Engineering, Dongguk University, Biometrics Engineering Research Center	Korea	0,0282
6	CATE	Department of Electrical and Computer Engineering, Florida International University	USA	0,0297
7	Dtibiolab	Biolab, Department of Information Technologies, University of Milan	Italy	0,0301
8	Font	Department of Electronic Engineering, Universidad Politécnica de Madrid	Spain	0,0305

NICE I: the winning algorithm (1)

- This algorithm has been presented by CASIA (National Laboratory of Pattern Recognition, Institute of Automation, Chinese Academy of Sciences)

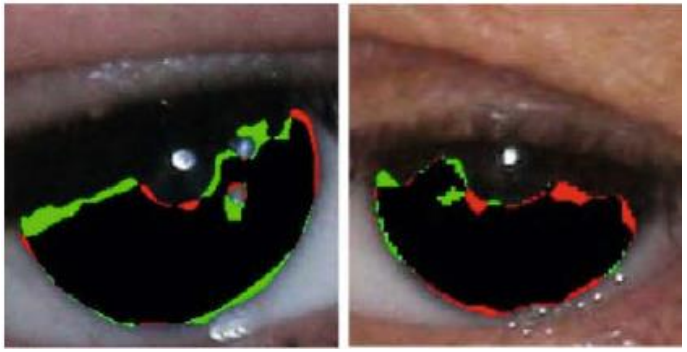

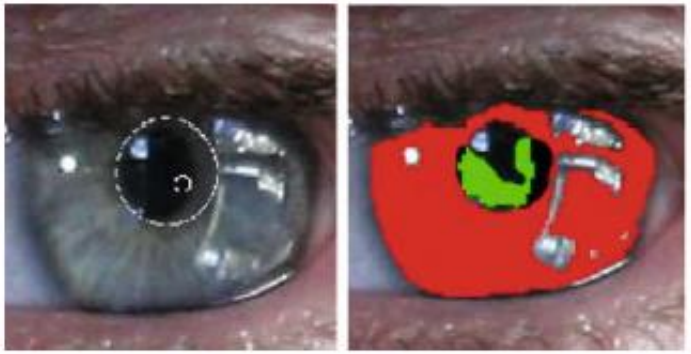

- Illustrations of successful segmentations (both images on the left) and inaccurate segmentations (the pair image-segmentation on the right, where light iris appears as skin)
- Green points denote false accept points (i.e. points labeled as noniris by the ground truth but iris by the method), the red points denote false reject points (i.e. points labeled as iris by the ground truth but non-iris by the method), and the black points are labeled as iris by both.

NICE I: the winning algorithm (2)

NICE I: the winning algorithm (2)

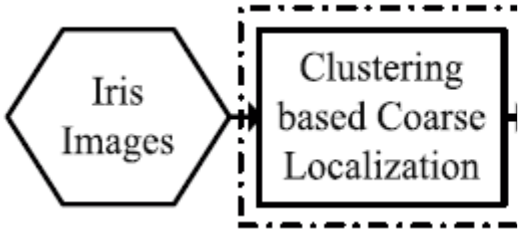

NICE I: the winning algorithm (2)

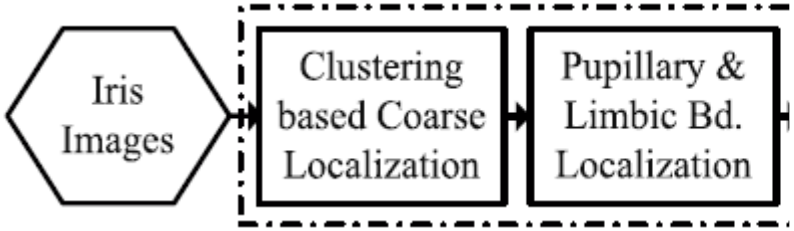

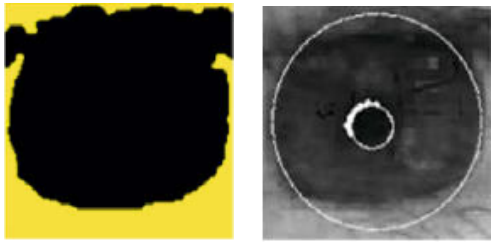

NICE I: the winning algorithm (2)

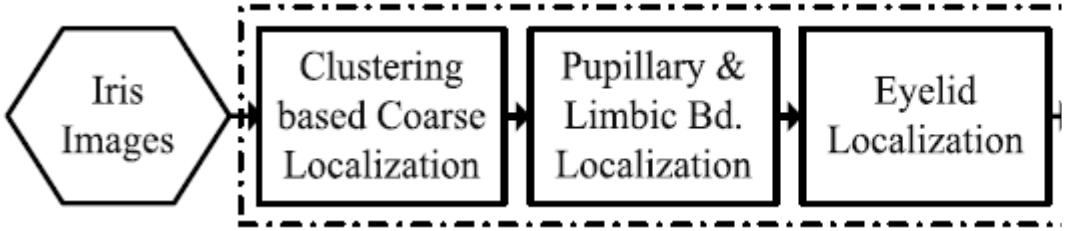

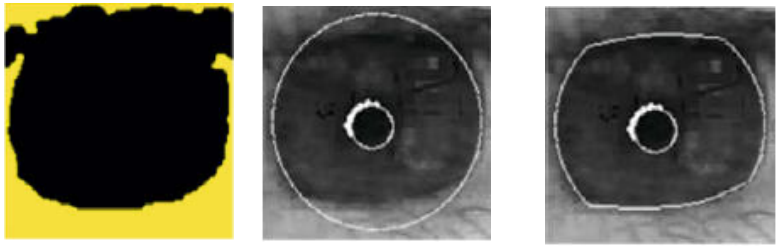

NICE I: the winning algorithm (2)

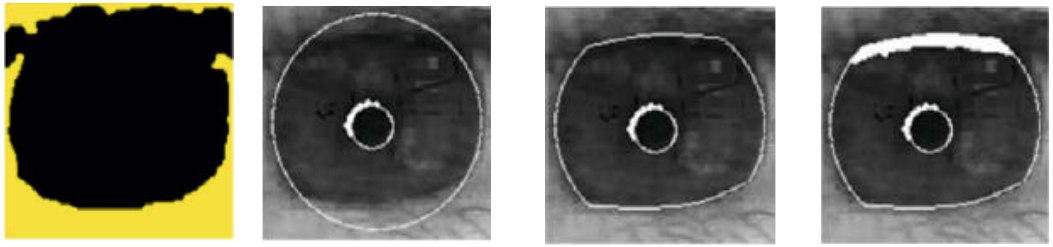

NICE I: the winning algorithm (2)

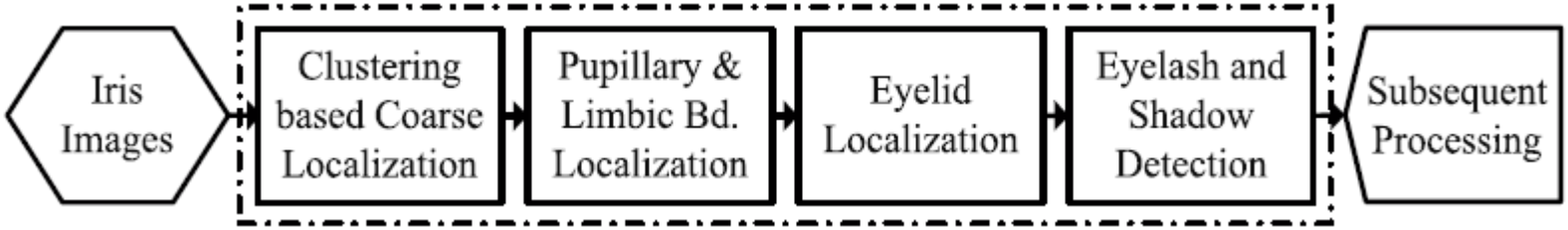

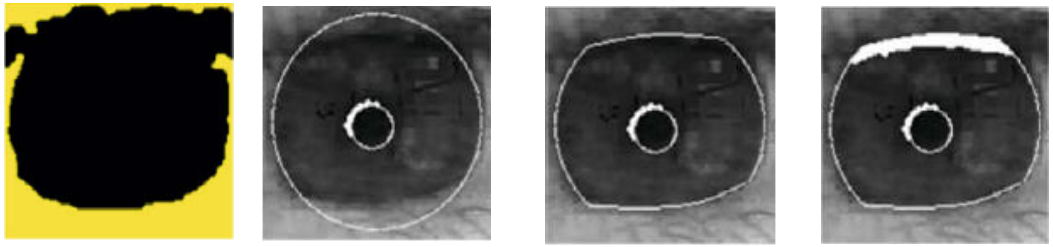

IS_{IS} steps and parameters

- IS_{IS} implies four main phases:
  - pre-processing
  - pupil location
  - linearization
  - limbus location
- All operative (e.g. image window sizes) and decision parameters (e.g. thresholds) have been experimentally tuned by using a separate training set of images

IS_{IS} Preprocessing

- Details of sclera vessels, skin pores, or eyelashes shape = complex patterns that can negatively interfere with edge detection
- A posterization filter *FE* (*Enhance*) is applied
  - a square window W is moved over the whole image, pixel by pixel
  - a histogram h_W is computed for the region in W
  - the value with the maximum occurrence is substituted for the central position.

Posterization: example

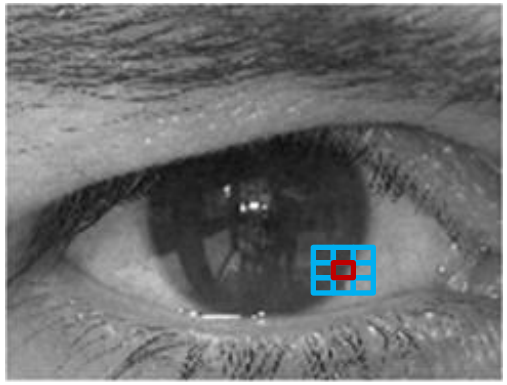

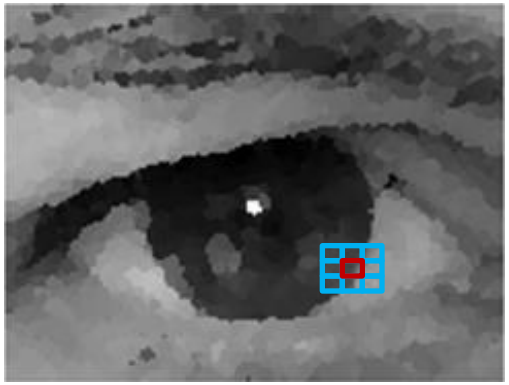

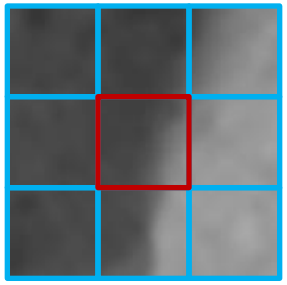

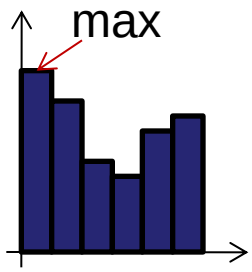

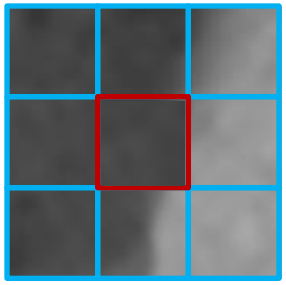

Canny filtering

- Canny filtering is applied with ten different thresholds *th=0.05,0.10,0.15,...,0.55*.

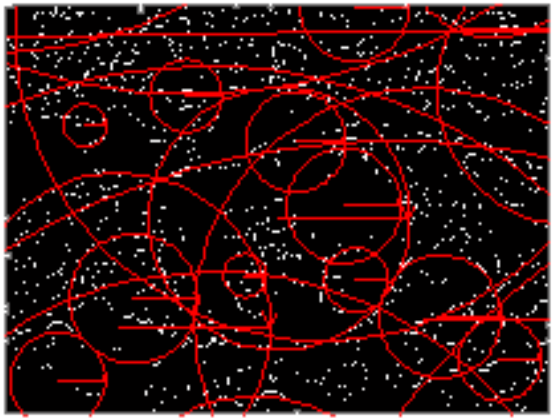

(a) th=0.05

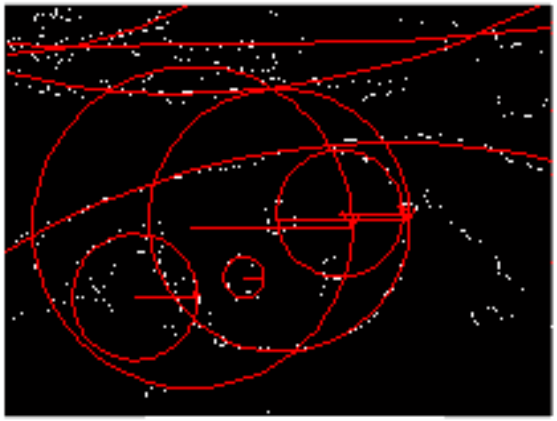

(b) th=0.15

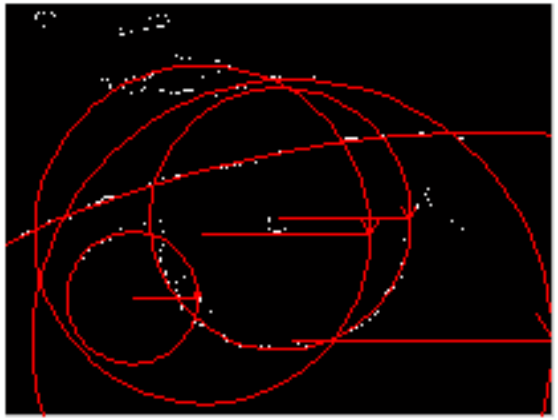

(c) th=0.35

Pupil location

- Many approaches search circular shapes through Hough transform or its adaptations = high computational cost

- Our algorithm detects circular objects using a precise and fast *circle detection* procedure presented by Taubin

Problems with ellipse fitting

- The presence of noise (e.g. spurious branches by Canny filter) may cause the erroneous detection of an elliptical shape even where the expected result would be a (quasi)circular one

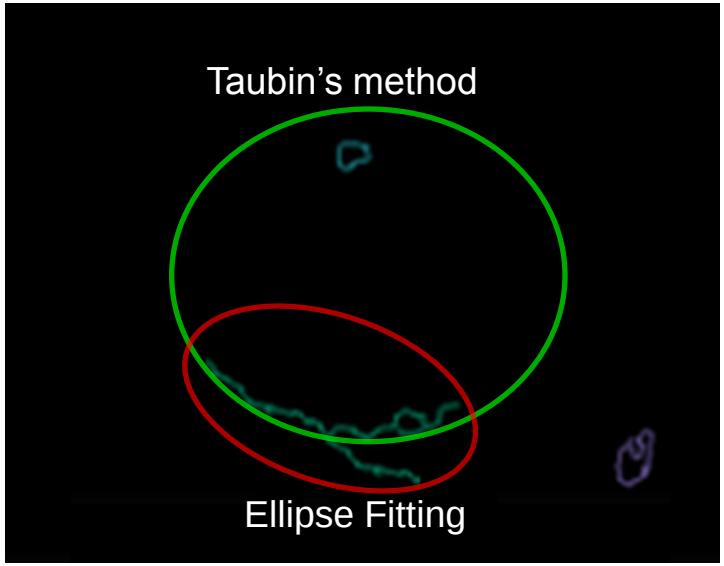

- The pupil is not a perfect circle, but searching for a circle causes a lower error than obtaining a noise-conditioned ellipse

Problems with Taubin

- Many circles are found while searching for the pupil
- Hough transform = tuning search parameters
- IS_{IS} = two ranking criteria to only select the best candidate pupil circle

Homogeneity: premise

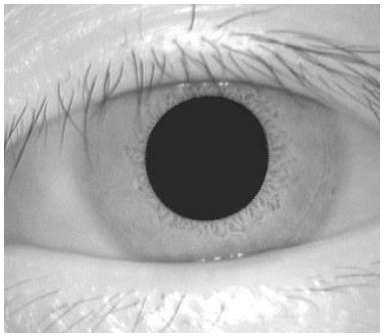

- In a number of approaches = darker region inside the image
- However, this is not always true
- In little controlled conditions = the pupil is often characterized by light reflections which alter its appearance

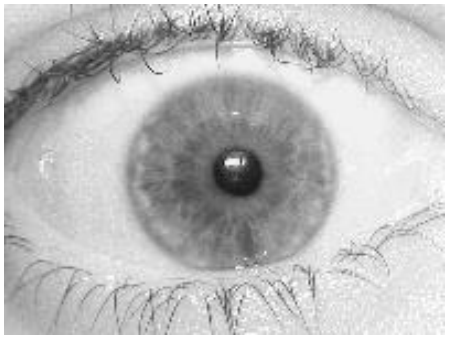

Homogeneity: example

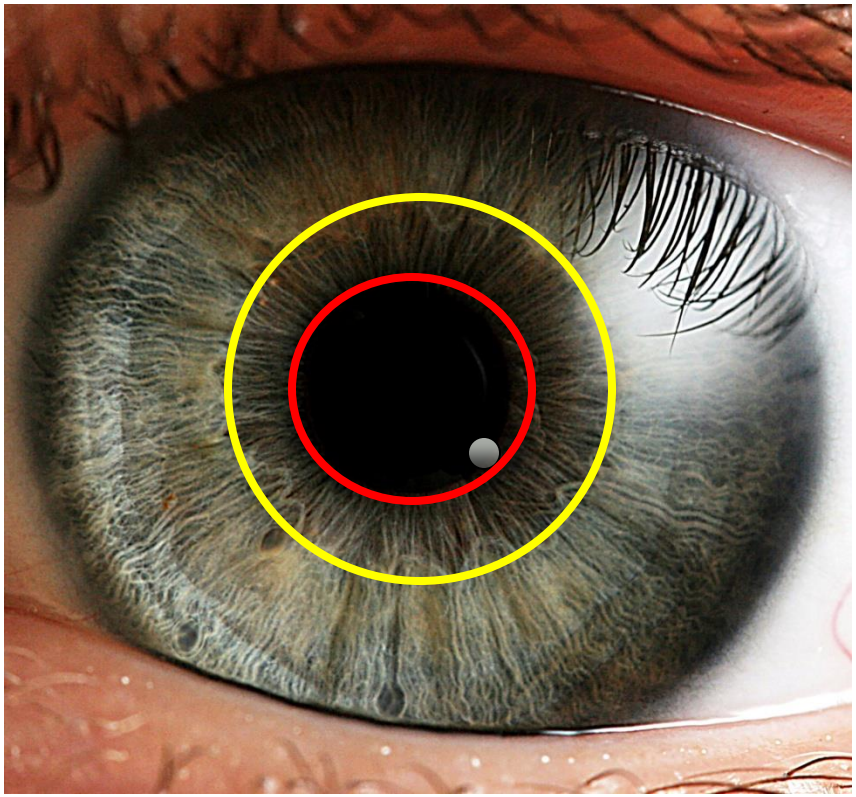

The best homogeneity score will be assigned to the inner circular region

Separability: premise

- Both limbus and pupil contour represent a boundary region with a pronounced step from a darker to a lighter zone
- Particularly dark irises are an exception, where such step is not so evident.

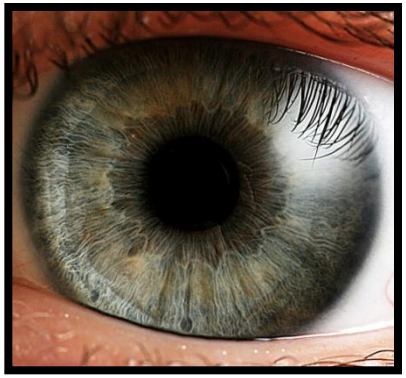

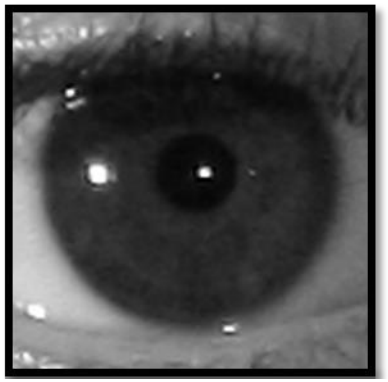

Separability

- Given a candidate circle C in L_C with centre $c=(c_x,c_y)$ and radius ρ in image I, the Cartesian coordinates are given by
  - $x_C(\rho,\theta)=c_x+\rho\cos(\theta)$
  - $y_C(\rho,\theta)=c_y+\rho\sin(\theta), \qquad \theta\in[0, 2\pi]$
- We consider the circle C_{IN} with radius $\rho_1=0.9\rho$ internal to C, and the circle C_{EX} with radius $\rho_2=1.1\rho$ external to C
- We measure the difference between the grey levels of corresponding pixels on such two circles for each angle θ_i around them

Separability: example

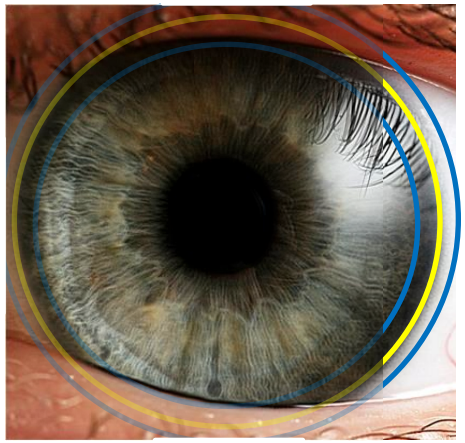

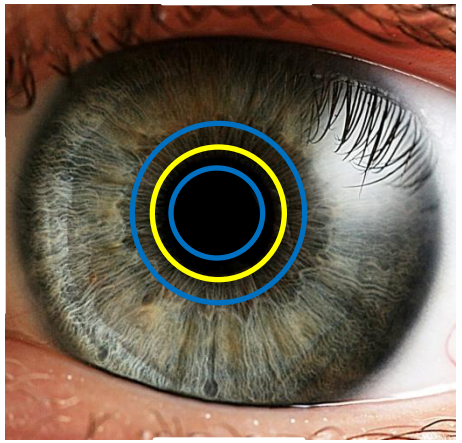

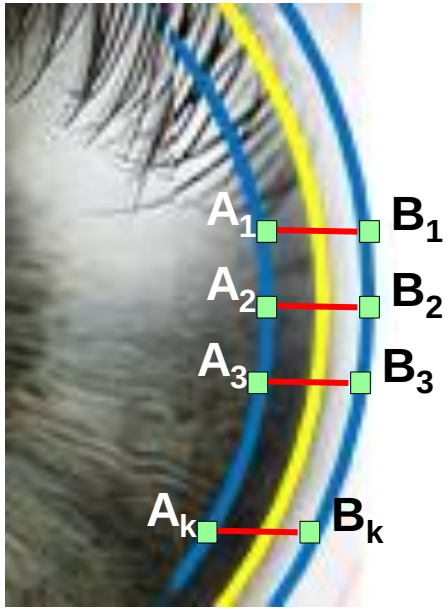

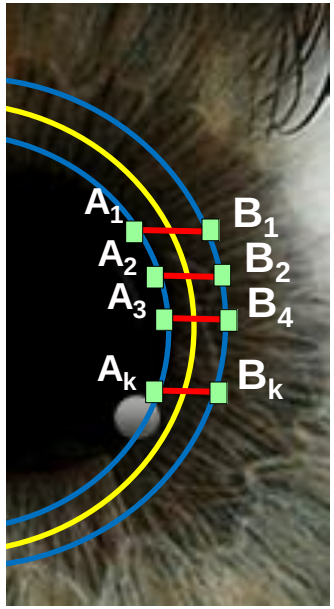

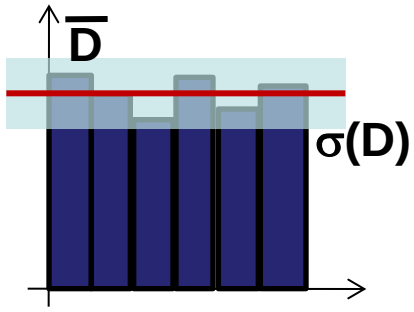

Pupil candidate selection

- Each circle in L_C undergoes the voting procedure, according to the *homogeneity* and *separability* criteria above
- The final score is

$$s = s_H + s_D$$

- The circle C_{max} with highest score s_{max} is considered as the circular shape which better approximates pupil

Linearization: example

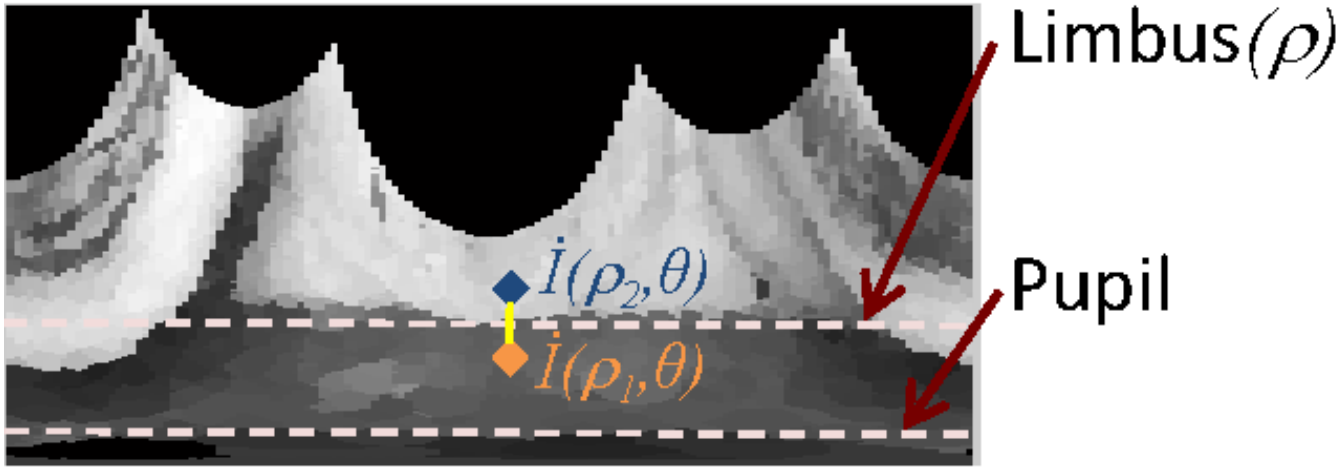

Along the vertical direction, it is possible to identify in an extremely precise way the limbo boundary region which separates iris from sclera

Limbus location

- For each column, ranging over ρ_j, and corresponding to a position θ_i of the horizontal axis of $\dot{I}$, we compute (pixel by pixel) the following weighted difference:

$$\Delta(\rho_j,\theta_i)=\varphi(\dot{I},\rho_j,\theta_i)\cdot\left(\dot{I}(\rho_j+\delta,\theta_i)-\dot{I}(\rho_j-\delta,\theta_i)\right)$$

- with

$$\varphi(\dot{I},\rho_j,\theta_i)=\begin{cases}1 & if \quad \dot{I}(\rho_j+\delta,\theta_i)-\dot{I}(\rho_j-\delta,\theta_i)>0 \\ & and \quad \min\left(\dot{I}(\rho_j-\delta,\theta_i),\dot{I}(\rho_j+\delta,\theta_i)\right)>\varepsilon_G \\ 0 & otherwise\end{cases}$$

Limbus location: example

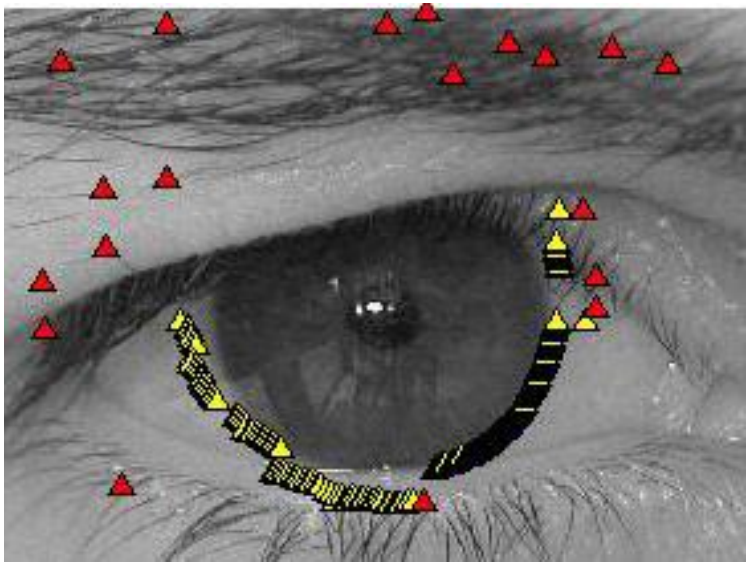

Limbus boundary *F* = points maximizing $\Delta(\rho_j, \theta_i)$ for each column θ_i in *İ*

Horizontal resolution of *İ* determines their number

What about yellow and red triangles?

Limbus location (continued)

- Points in F belong to a polar space = their ρ component should remain about constant while θ describes an approximate circle
- Smoothness criterion = avoid outliers
- We compute the median value value ρ_{med} over F, and compute a relative error

$$err = \frac{\left|\rho_i - \rho_{med}\right|}{\max_i \left|\rho_i - \rho_{med}\right|}$$

Limbus location (continued)

- Points in F with a ρ_i producing a relative error above a threshold ε are cancelled (red points)

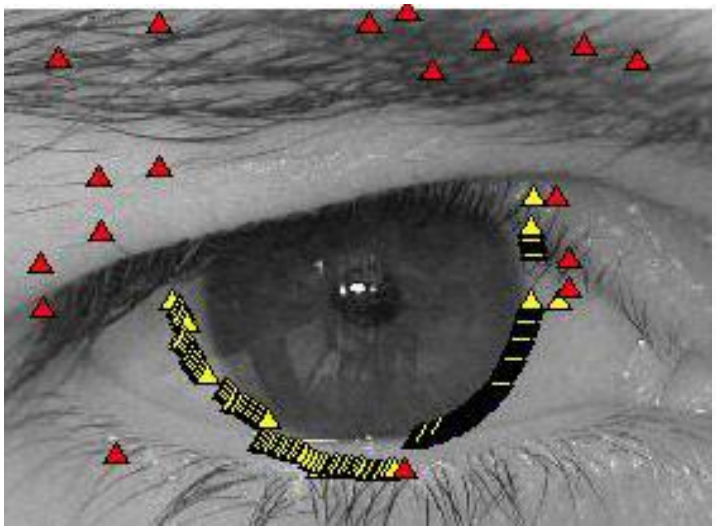

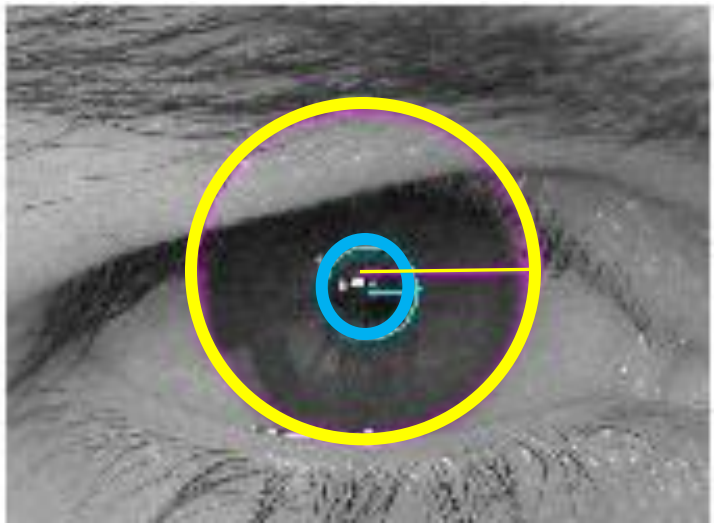

Experimental results

- Test databases = CASIA v3 Lamp and UBIRIS v1 Session 2

- CASIA images = 640x480 resolution
- UBIRIS images = 800x600

- Comparison with a system built from Masek's implementation of iris-related algorithms = segmentation follows the Wildes' method, recognition follows the Daugman's approach
- Both segmentations are compared with a precise manual one

- IS_{IS} = it was not necessary to adapt any of the thresholds
- Other methods = it was necessary to adapt the parameters to the single database

Experimental results: examples

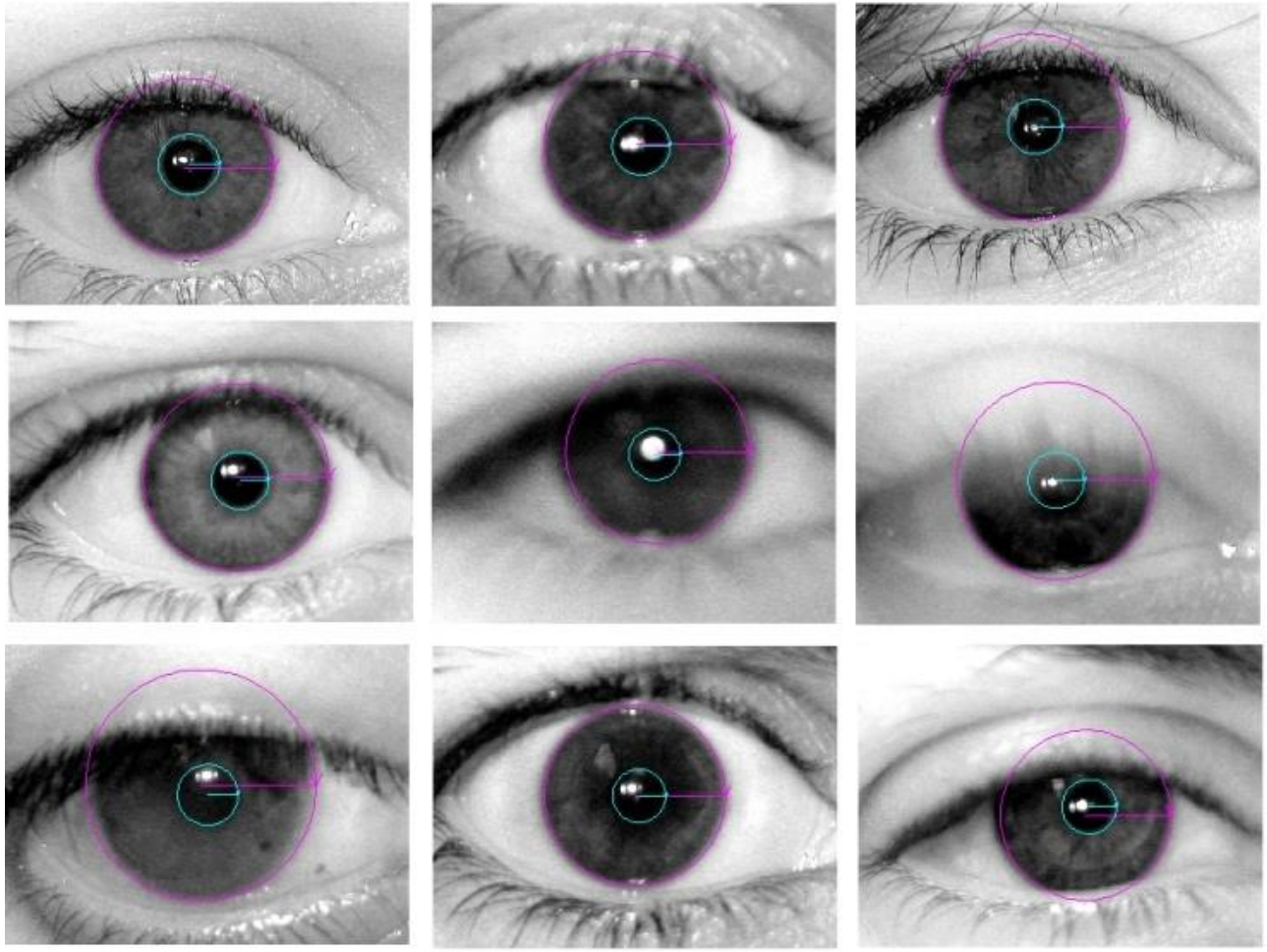

N-IRIS recognition system

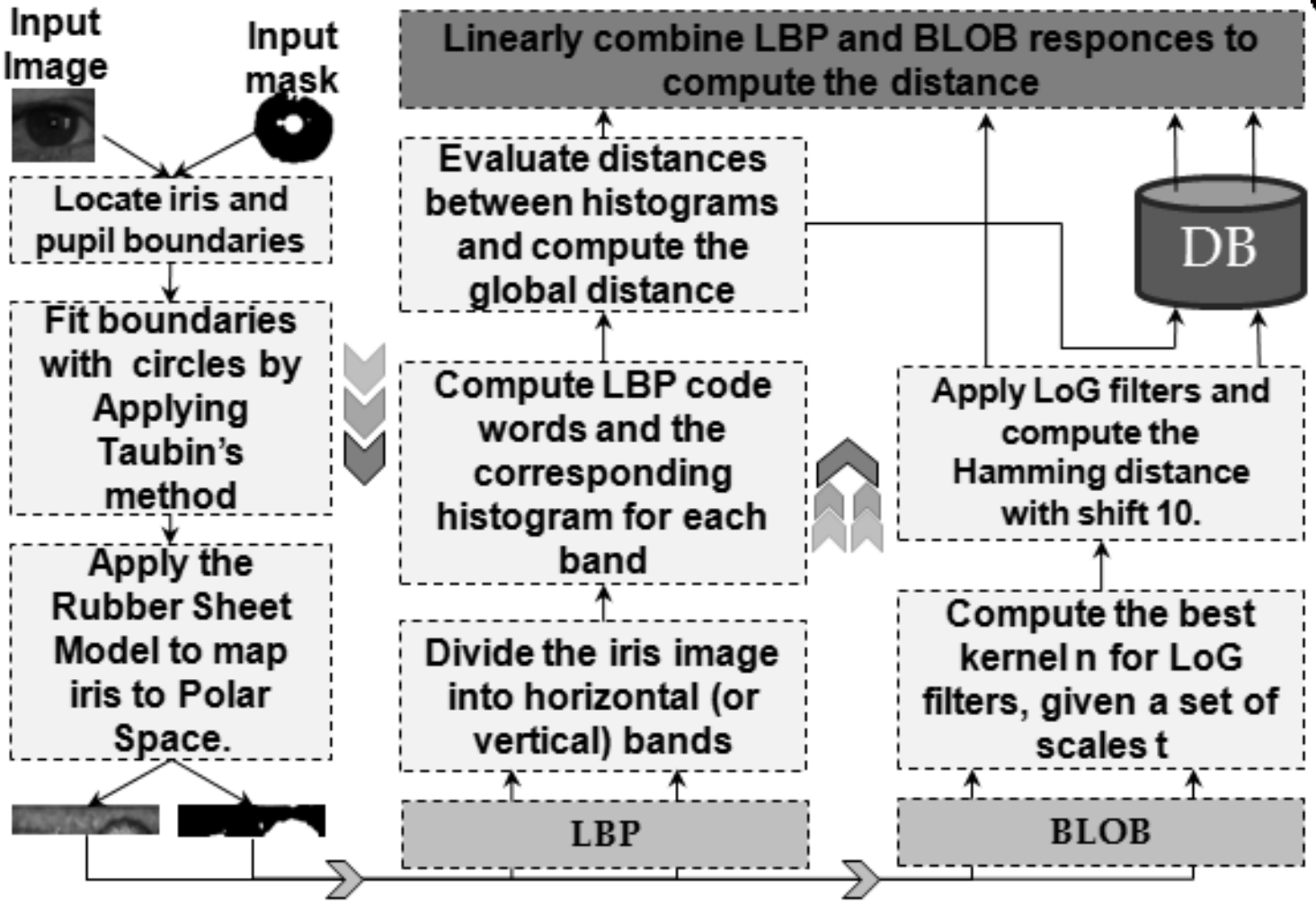

Coding and matching

- **Coding**
  - **Input:**
    - Normalized iris and mask
  - **Output:** coding
  - **Function:** create a biometric template
- **Matching**
  - **Input:**
    - Probe coding, gallery coding
  - **Output:** distance value
  - **Funzione:** compute the lowest distance

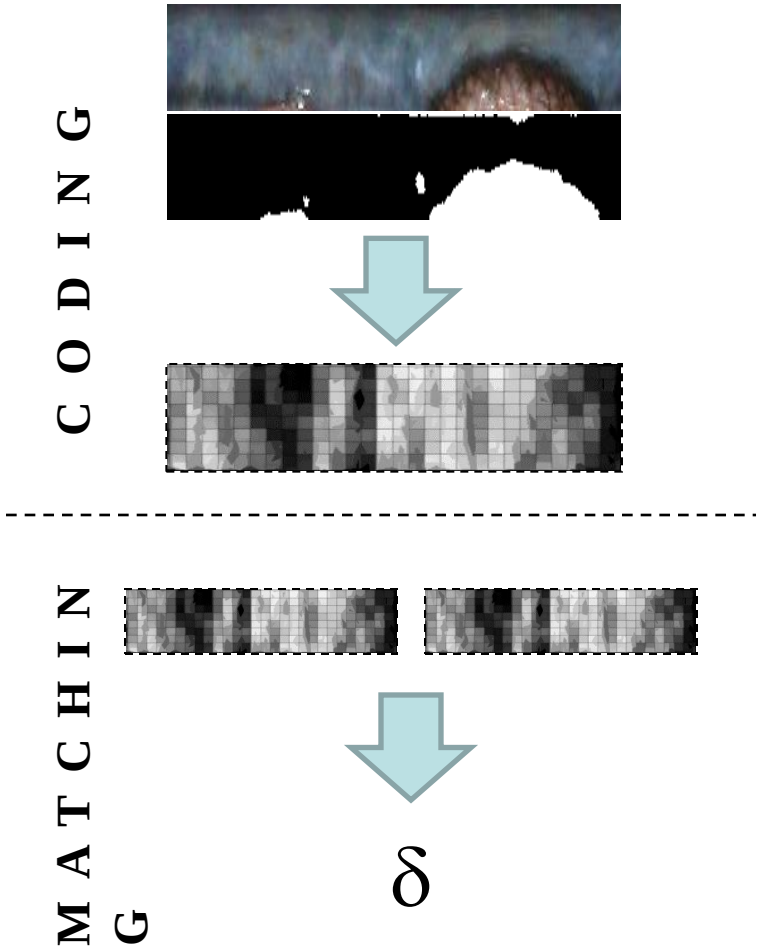

Iris features: texture

- Iris texture

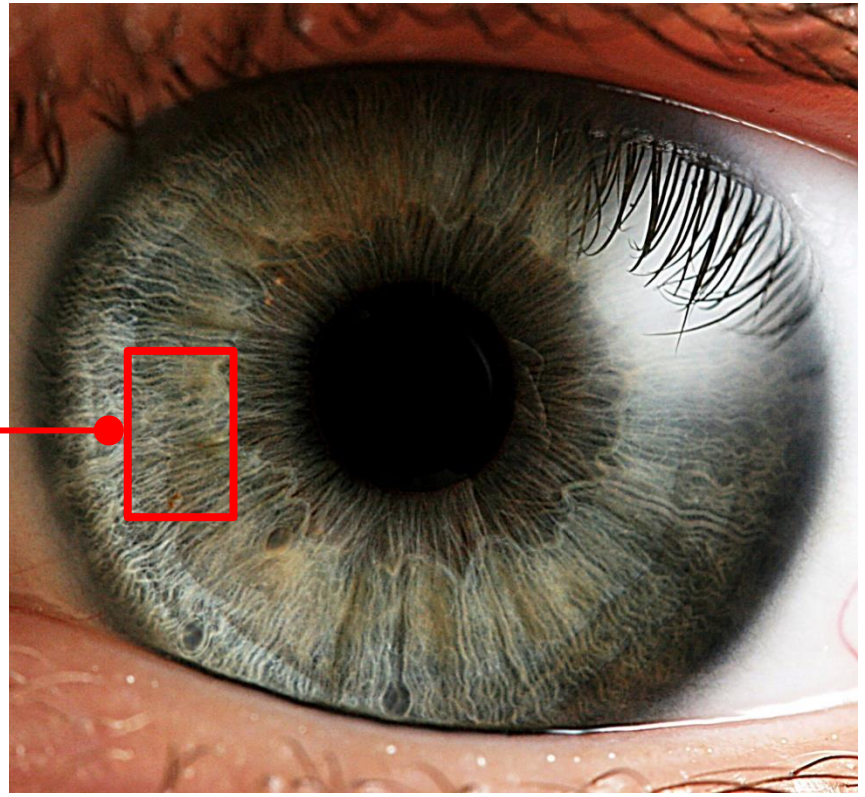

LBP

- **LBP = Local Binary Pattern**
- Analisys of textural regularities

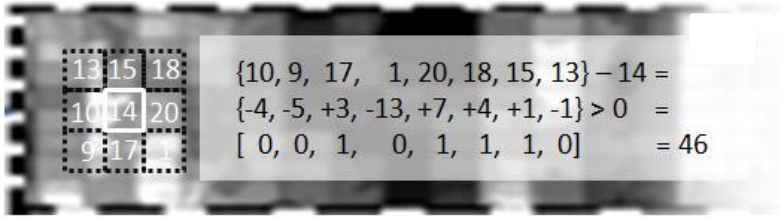

Neighborhood of 8 elements -> 256 values

Histogram of values represents the texture

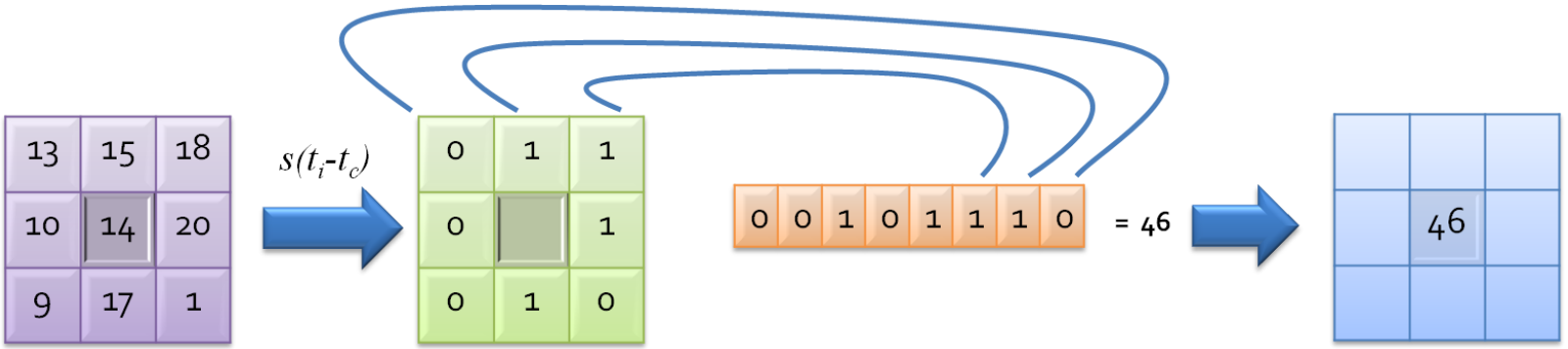

LBP for iris

- Sun et al.* divide the normalized iris in blocks.
- We tried the division in horizontal (anatomically meaningful) or vertical bands.

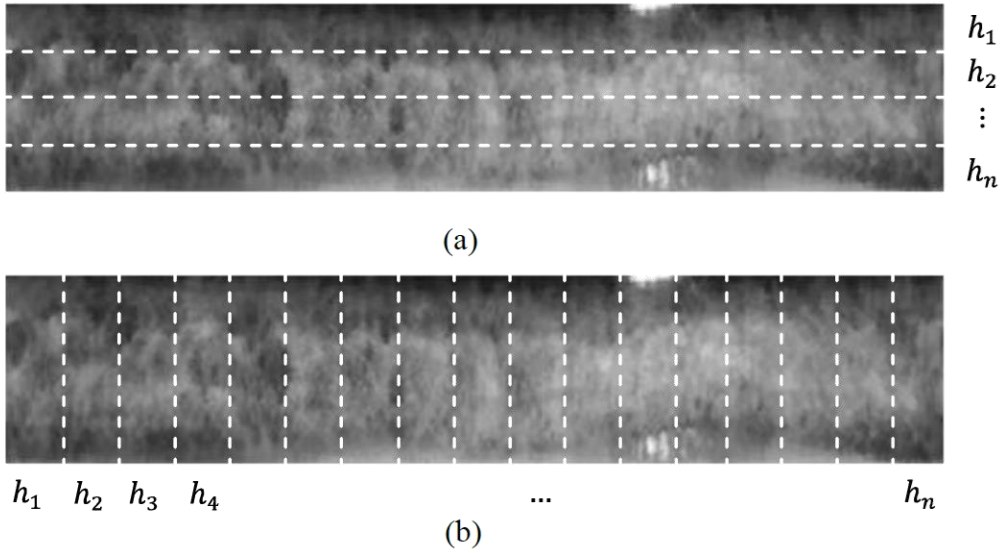

Code= Set of histograms + Mask

*Sun Z., Tan T., Qiu X., 2006. Graph Matching Iris Image Blocks with Local Binary Pattern. In Proceedings of the International Conference on Biometrics, pp.366–372

Matching for LBP

Matching:

- given $C = (H_1, H_2, \ldots, H_n, M) \quad P = (K_1, K_2, \ldots, K_n, N)$
- given a measure of similarity between histograms δ
- similarity between codes will be:

$$\frac{1}{n}\sum_{i=1}^{n}\delta(H_i, K_i)\left(1 - \frac{\overline{noise}_i}{totpixel}\right)$$

- As we will see from results:
  - Horizontal division better than vertical one
  - No too narrow bands

Iris features: blobs

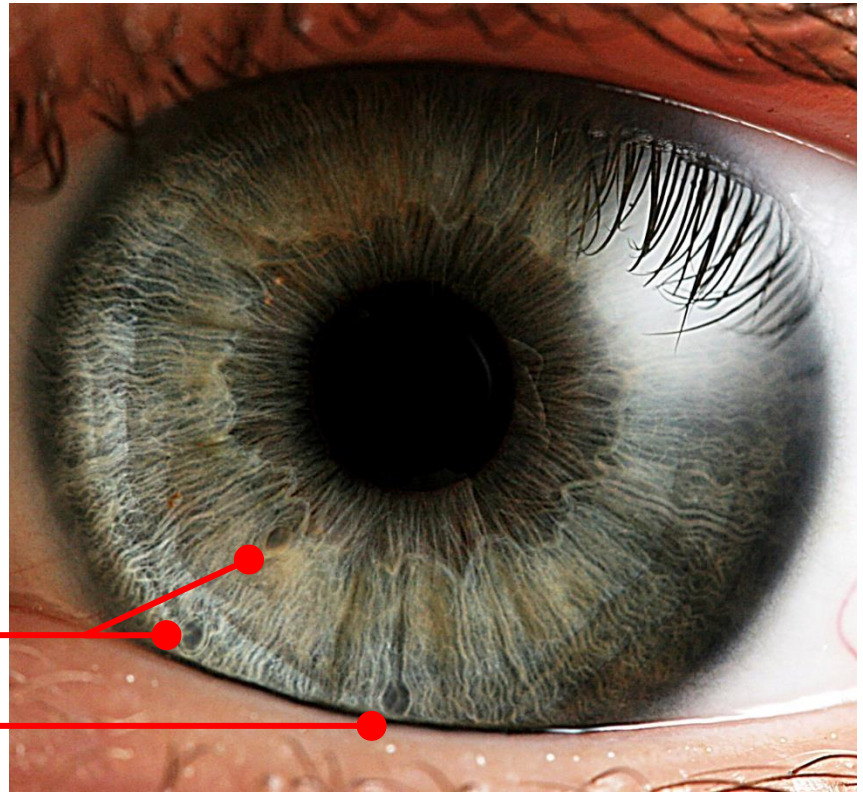

- Blobs

Iris features: blobs

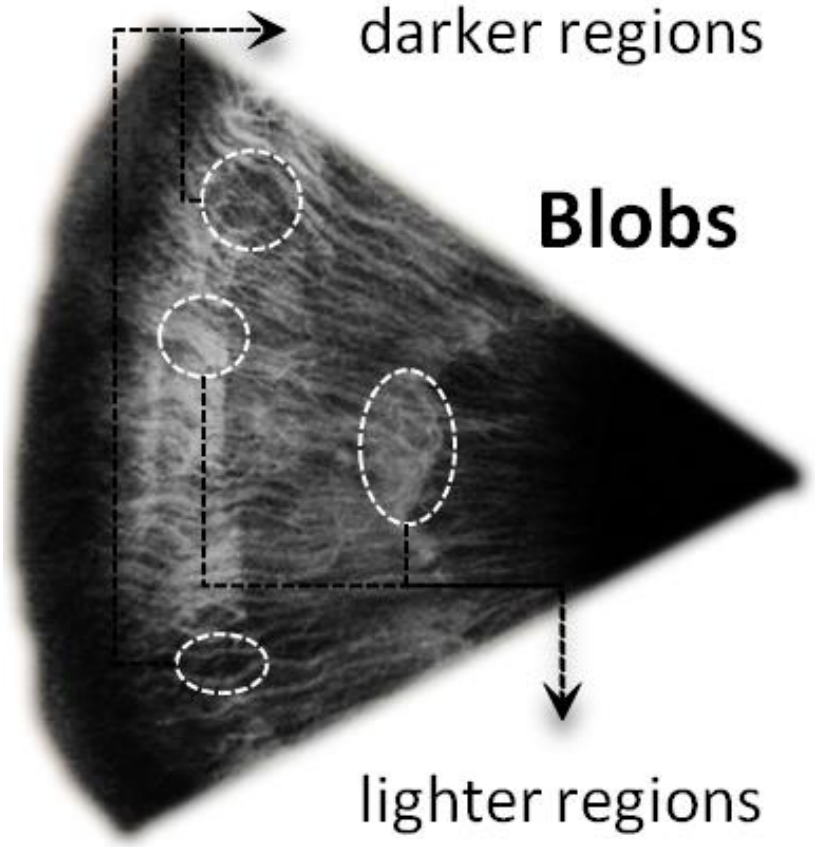

Blob detection

- ❖ Furrows and crypts make up the blobs
- ❖ Use of Laplacian of Gaussian (LoG)*

- Gaussian:

$$f(x,y) = \frac{1}{\sqrt{2\pi t}} e^{-\frac{x^2+y^2}{2t}}$$

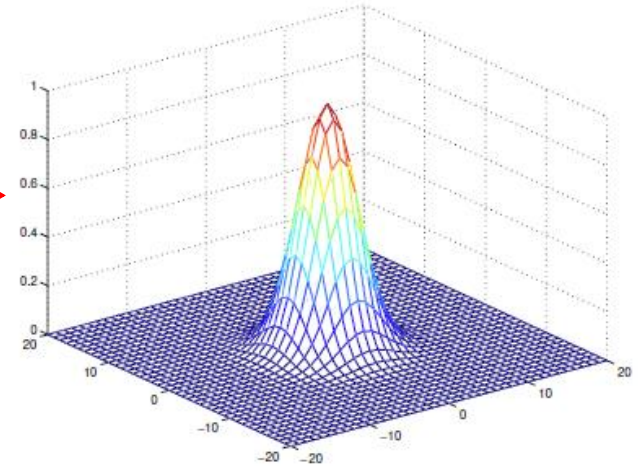

- Laplacian:
  - 2° order differential operator
  - 2D is defined by:

$$\Delta = \nabla^2 = \frac{\partial^2}{\partial x^2} + \frac{\partial^2}{\partial y^2}$$

*Chenhong L., Zhaoyang L., 2008. Local feature extraction for iris recognition with automatic scale selection. Image and Vision Computing, vol. 26, no. 7, pp. 935–940.

Blob detection

- Different scales
- Normalization

$$\nabla^2_{\text{norm}} f = t \cdot (\nabla^2 f)$$

- Fusion:
  - Point with higher LOG
- Binarization
- Matching = Hamming distance weighted by segmentation mask
- N-IRIS also considers shifts of 10 pixels -> the final distance = computed on the alignment returning the maximum match

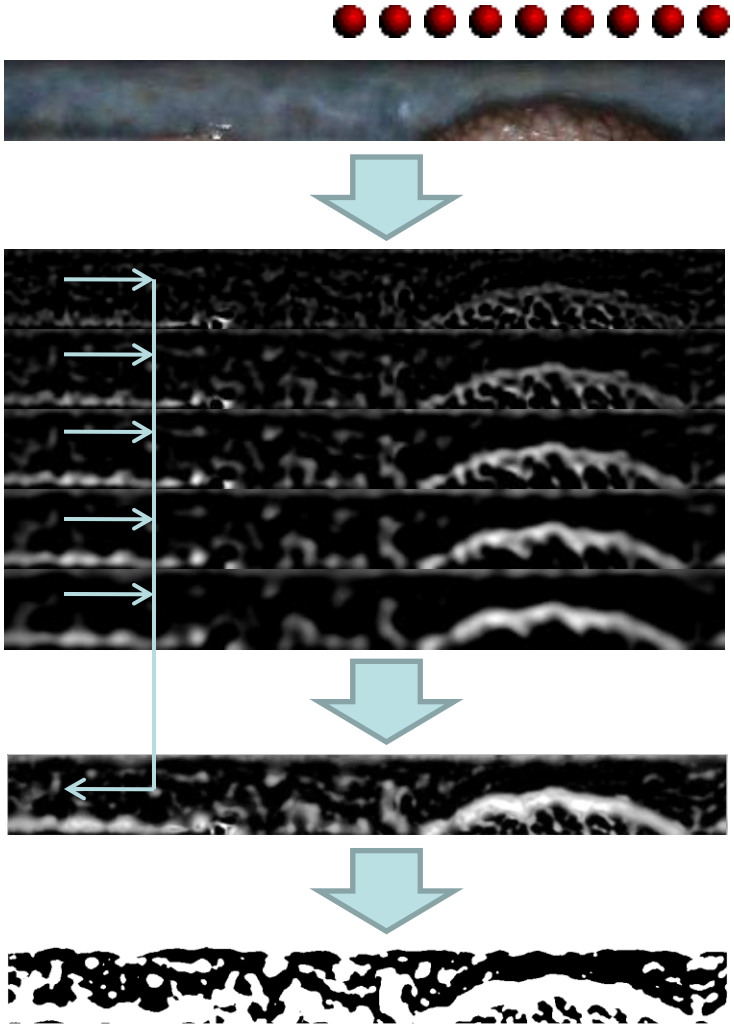

Blob detection: a variation

- Scales are not fused but chained
- Matching: mean Hamming distance

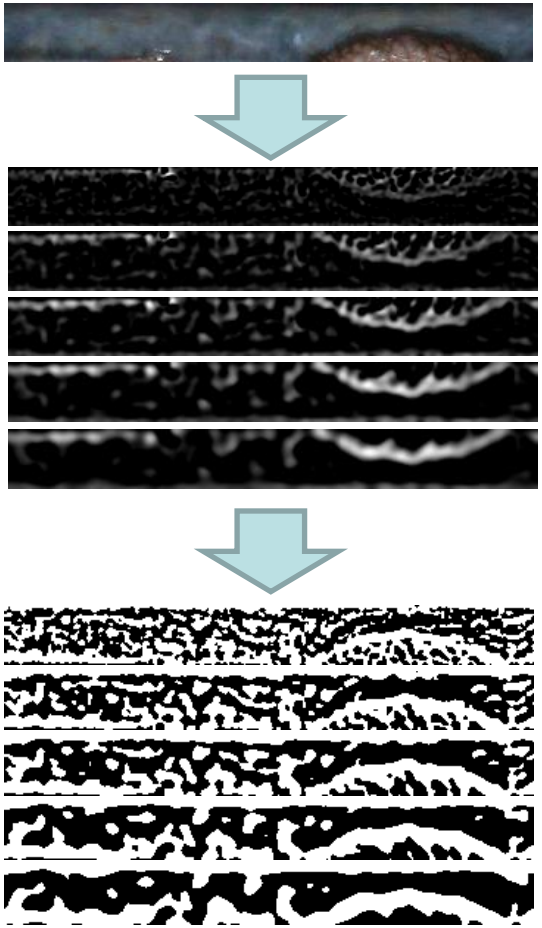

LBP-Blob

- **LBP-BLOB** fuses the two methods
- How are they fused?
  - Codings are chained
  - Matching given by: $c = \{c^{LBP}, c^{BLOB}\}$

$$\delta(c_1, c_2) = \frac{\delta_{LBP}(c_1^{LBP}, c_2^{LBP}) + \delta_{BLOB}(c_1^{BLOB}, c_2^{BLOB})}{2}$$

- **What do we expect:**
  - $\exists$ images for which one method is better than the other …
  - … then LBP-BLOB is expected to work generally better than the single ones!

LBP(ROC,CMC,ERR) on UBIRIS.v2

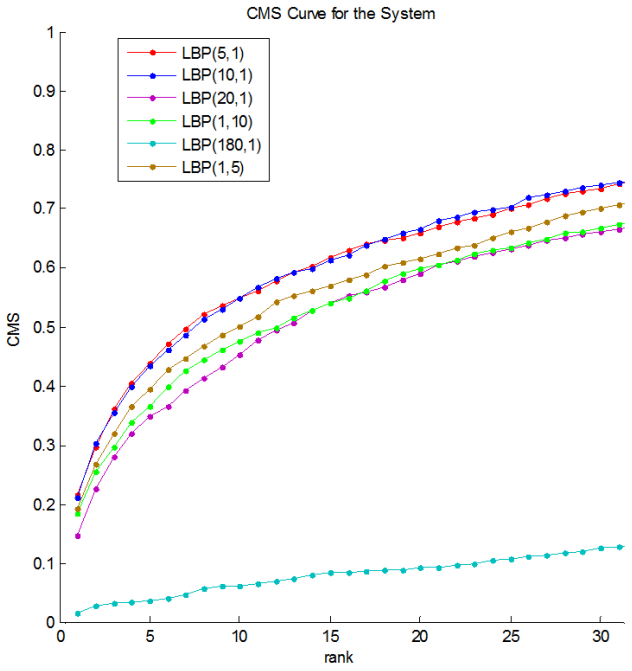

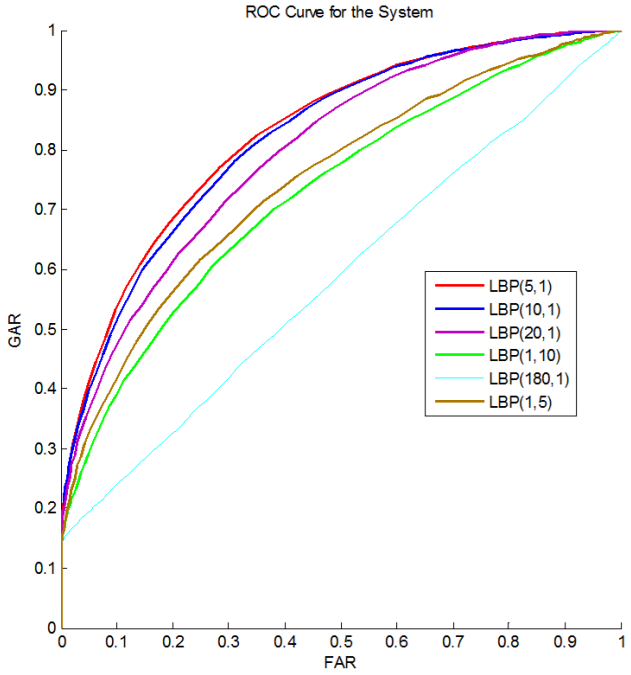

Configurazione	ERR %
LBP(5,1)	0.26
LBP(10,1)	0.27
LBP(20,1)	0.29
LBP(1,10)	0.34
LBP(1,180)	0.45
LBP(1,5)	0.32

- LBP(n,m) = LBP execution on an image subdivided in n columns and m rows.
- Horizontal bands (m=1) work better

BLOB(ROC,CMC,ERR) on UBIRIS.v2

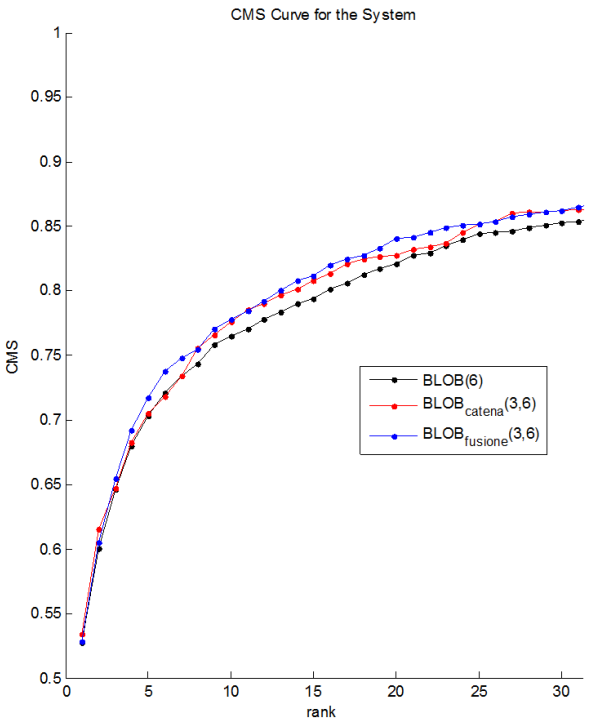

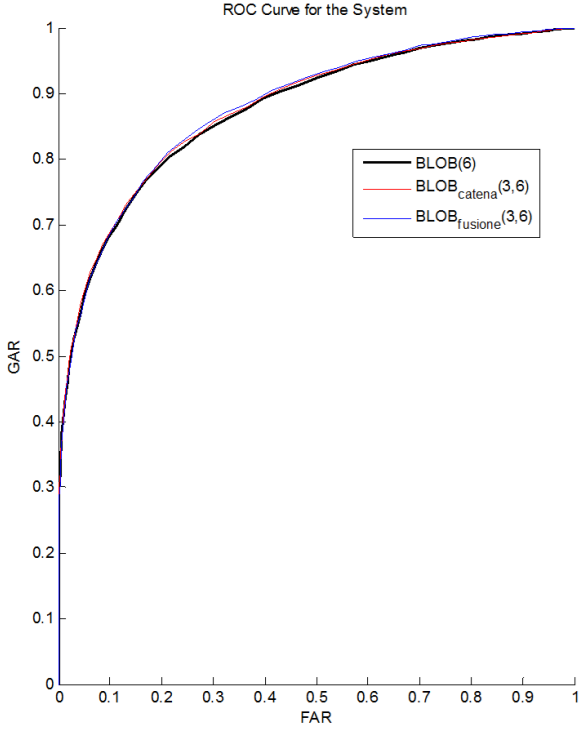

Configurazione	ERR %
BLOB(4)	0.19
BLOB(3,6, chain)	0.20
BLOB(3,6, fusion)	0.20

- BLOB(t1) will denote single scale execution of BLOB at scale t1
- BLOB(t1, t2, mode) will denote the execution of BLOB in mode {chain, fusion} for the pair of scales (t1, t2)
- For UBIRIS.v2 single scale worked better

LBP- BLOB(ROC,CMC,ERR) on UBIRIS.v2

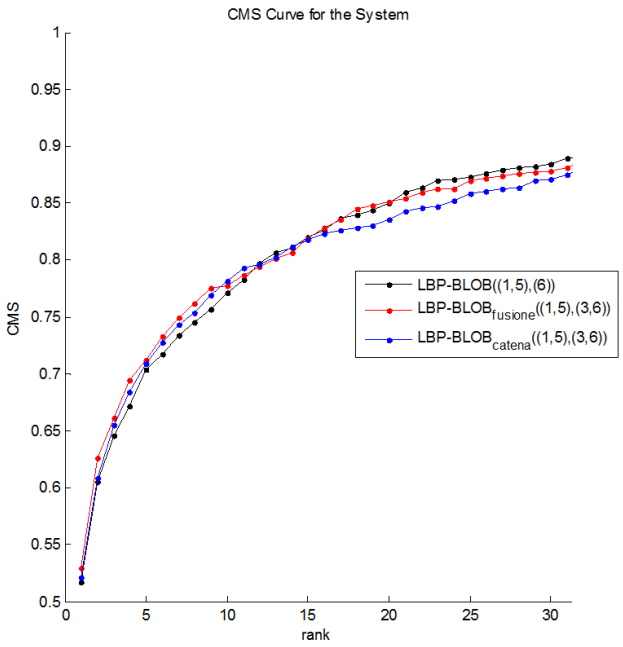

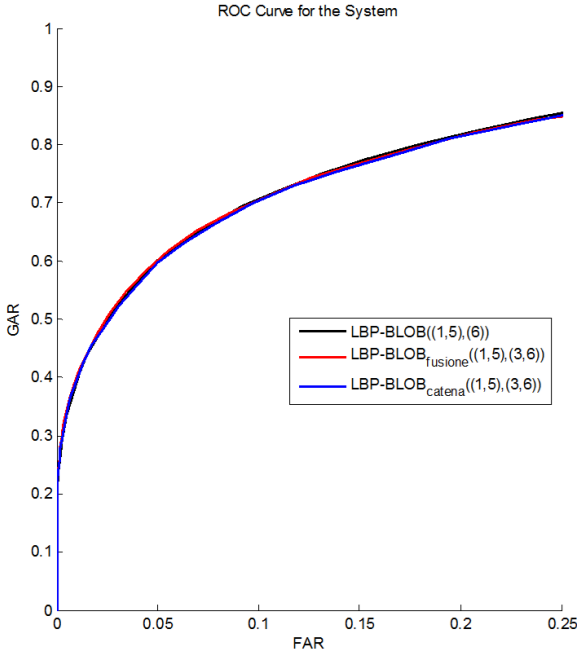

Configurazione	ERR %
LBP-BLOB(6)	0.19
LBP-BLOB(5,1,3,6, chain)	0.20
LBP-BLOB(5,1,3,6, fusion)	0.19

LBP- BLOB(ROC,CMC,ERR) on NICE II tuning dataset

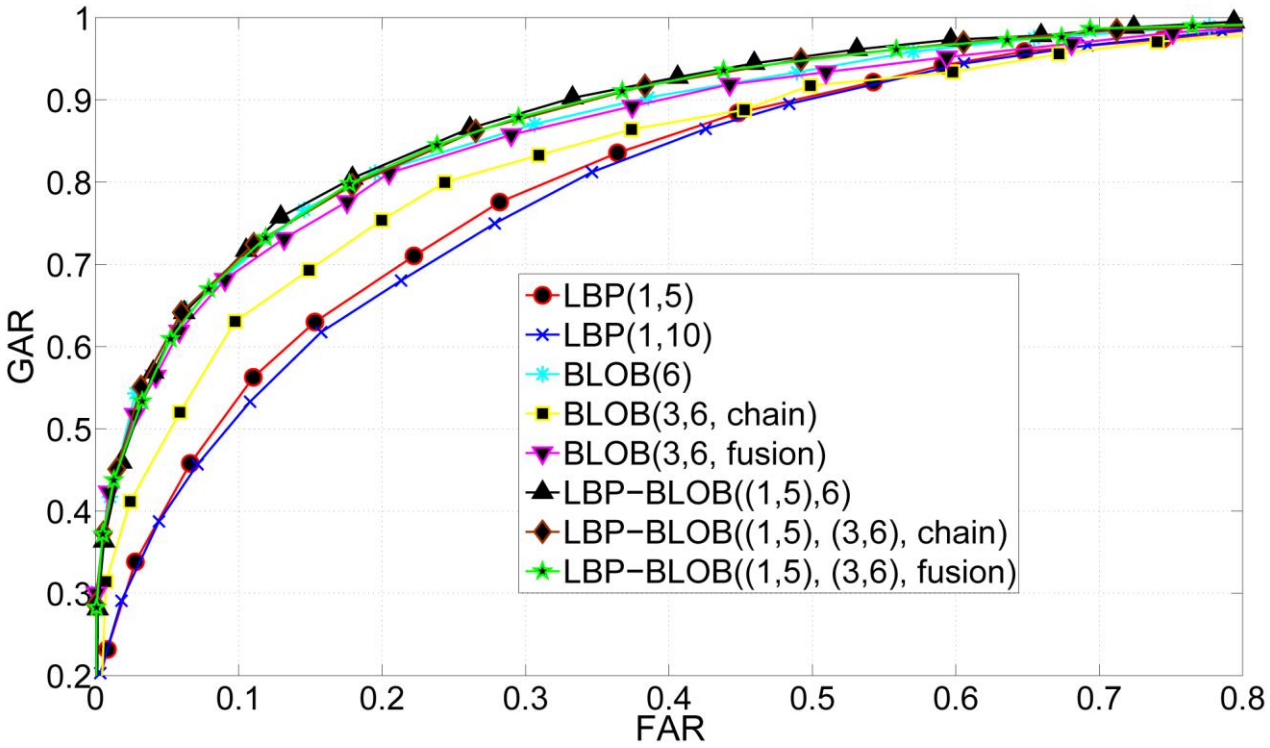

NICE II

NICE II Committees

Contest Chairs:

- **Hugo Proença**, Department of Computer Science, SOCIA Lab., IT-Networks and Multimedia Group, University of Beira Interior.
- **Luís A. Alexandre**, Department of Computer Science, SOCIA Lab., IT-Networks and Multimedia Group, University of Beira Interior.

Organizing Committee:

- **David Carvalho,** Department of Computer Science, University of Beira Interior.
- **João Oliveira,** Department of Computer Science, SOCIA Lab., University of Beira Interior.
- **Gil Santos,** Department of Computer Science, SOCIA Lab., University of Beira Interior.
- **Sílvio Filipe,** Department of Computer Science, SOCIA Lab., University of Beira Interior.

NICE II (2)

- NICE II received a total of 67 participants from over 32 countries.
- **June 30th, 2010**: The deadline for the final submission of the participations
- **July 15th, 2010:** The classification of the best participants is available.

NICE II (3)

The Protocol

- The submitted application executable can be written in any programming language and must run in standalone mode, in one of the operating systems:”Windows XP, Service Pack 2” or ”Fedora Core 6”.

- There will be no internet access during the NICE.II evaluation. Thus, the application executable will need to be installed and executed without access to the internet.

NICE II (4)

Let **P** denote the submitted application, which gives the dissimilarity between segmented iris images.

Let $\mathbf{I}=\{\mathbf{I_1},\ldots,\mathbf{I_n}\}$ be the data set containing the input iris images an let $\mathbf{M}=\{\mathbf{M_1},\ldots,\mathbf{M_n}\}$ be the corresponding binary maps that give the segmentation of the noise-free iris region.

P receives two iris images (and the corresponding binary maps) and outputs the dissimilarity value between the corresponding irises: $\mathbf{P(I_i, M_i\ I_j, M_j)} \dashrightarrow \mathbf{D}$. **D** should be a real positive value.

Performing a "one-against-all" comparison scheme for each image of **I** gives a set of intra-class dissimilarity values $\mathbf{D^I}=\{\mathbf{D^I_1},\ldots,\mathbf{D^I_k}\}$ and a set of inter-class dissimilarity values $\mathbf{D^E}=\{\mathbf{D^E_1},\ldots,\mathbf{D^E_m}\}$, whether the captured images are from the same or from different irises.

The decidability value $\mathbf{d'(D^I_1,\ldots,D^I_k,D^E_1,\ldots,D^E_m)} \dashrightarrow \mathbf{[0,\ \infty[}$ will be used as evaluation measure:

$$\mathbf{d'=|\ avg(D^I)\ -\ avg(D^E)|\ /\ sqrt\ (\ 0.5*\ (\ std(D^I)^2\ +\ std(D^E)^2)\ )}$$

where $\mathbf{avg(D^I)}$ and $\mathbf{avg(D^E)}$ denote the average values of the intra-class and inter-class comparisons and $\mathbf{std(D^I)}$ and $\mathbf{std(D^E)}$ the corresponding standard deviation values.

Participants of the NICE:II contest will be ranked from the highest (best) to the lowest (worst) decidability values.

NICE II (5)

- The participants that achieved the best 8 results were invited to publish their approach in a Special Issue *NICE II NOISY IRIS CHALLENGE EVALUATION PART II*, *Pattern Recognition Letters*, (Elsevier),vol 33, n° 8, 2012

Ranking	Unsername	Affiliation	Country	Decidability (d')
1	CASIA	National Laboratory of Pattern Recognition, Institute of Automation, Chinese Academy of Sciences	China	2,5748
2	Betaeye	Techshino Biometrics Research Center,Department of Mathematics, Northeastern University	China	1,8213
3	UBI	University of Beira Interior	Portugal	1,7786
4	Parkgr	Biometrics Engineering Research Center (BERC), Dongguk University	Republic of Korea	1,6398
5	PeihuaLi	College of Computer Science and Technology, Heilongjiang University	China	1,4758
6	BIPLab	University of Salerno	Italy	1,2565
7	HLJUCS	College of Computer Science and Technology, Heilongjiang University	China	1,1892
8	DMCS	Technical University of Lodz	Poland	1,0931

NICE II: the winning algorithm (1)

- This algorithm has been presented by CASIA (National Laboratory of Pattern Recognition, Institute of Automation, Chinese Academy of Sciences)

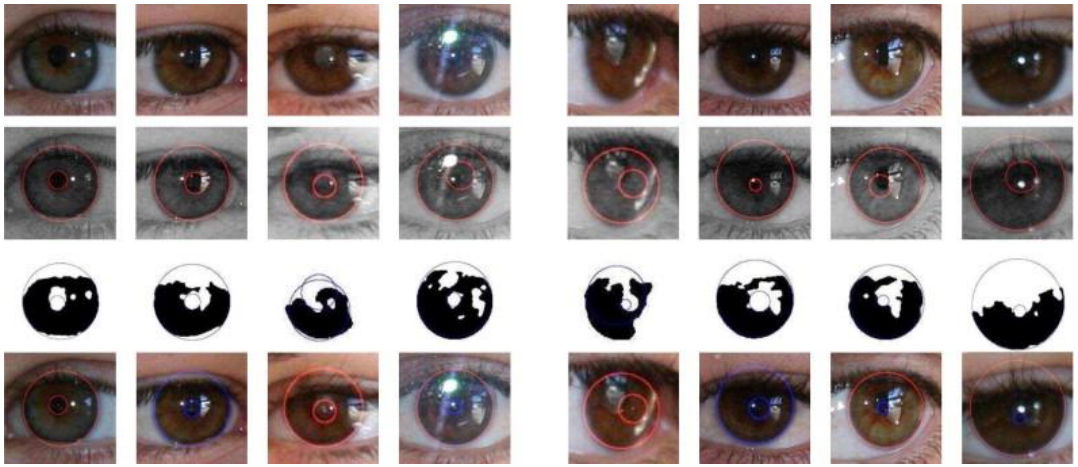

NICE II: the winning algorithm (2)

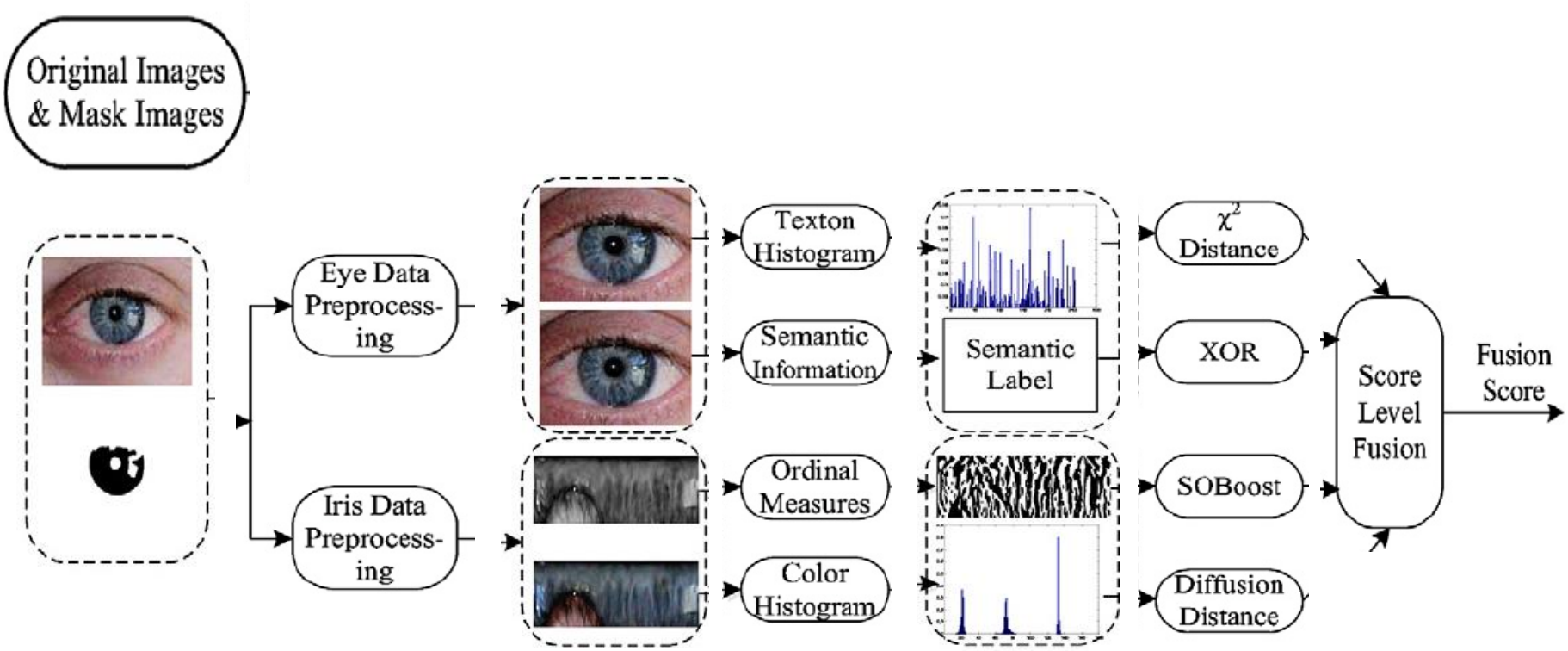

Some readings

- J. Daugman, "High Confidence Visual Recognition of Persons by a Test of Statistical Independence", *IEEE Transactions on Pattern Analysis and Machine Intelligence*, vol. 15, no. 11, pp. 1148-1161, 1993.
- J. Daugman, "Biometric Personal Identification System Based On Iris Analysis", US Patent 5291560, 1994.
- R. Wildes (1994) A system for automated iris recognition IEEE Workshop on Applications of Computer Vision, pp. 121-128.
- J. Daugman, "Statistical Richness of Visual Phase Information: Update on Recognizing Persons by Iris Patterns", *International Journal of Computer Vision*, vol. 45, no. 1, pp. 25-38, 2001.
- J. Daugman (2004). How Iris Recognition Works. IEEE Transactions on Systems for Video Technology, vol. 14, no. 1, pp. 21-30.
- H. Proença, L. A. Alexandre (2007). The NICE.I: Noisy Iris Challenge Evaluation – Part I. *IEEE First International Conference on Biometrics: Theory, Applications and Systems*
- Z. He, T. Tan, Z. Sun, X. Qiu (2008). Towards Accurate and Fast Iris Segmentation for Iris Biometrics. IEEE Transactions on PAMI, vol. 31, no. 9, pp. 1670-1684.
- 2010 A. Abhyankar, S. Schuckers (2010) A novel biorthogonal wavelet network system for off-angle iris recognition. Pattern recognition, vol. 43, no. 3, pp 987-1007.
- T. Tan, Z. He (2010). Efficient and robust segmentation of noisy iris images for non-cooperative iris recognition. Image and Vision Computing, vol. 28, no. 2, pp. 223-230.

Some readings

- H. Proença, L. A. Alexandre (2012). Toward Covert Iris Biometric Recognition: Experimental Results From the NICE Contests. IEEE Transactions on Information Forensics and Security, vol. 7, no. 2, pp. 798-808
- Handbook of Iris Recognition (2012) (eds.) Springer M. De Marsico, M. Nappi, D. Riccio (2010). ISIS: Iris Segmentation for Identification Systems International Conference on Pattern Recognition, pp. 2857-2860.
- M. De Marsico, M. Nappi, D. Riccio, H. Wechsler (2011) Iris Segmentation Using Pupil Location, Linearization, and Limbus Boundary Reconstruction in Ambient Intelligent Environments Journal of Ambient Intelligence and Humanized Computing, vol. 2, no. 2, pp. 153-162.
- M. De Marsico, D. Riccio (2012). Iris Recognition in Visible Light Domain. International Conference on Pattern Recognition, Applications and Methods, pp. 55-62, 2012. 2012
- M. De Marsico, M. Nappi, D. Riccio (2012). Noisy Iris Recognition Integrated Scheme. Pattern Recognition Letters, vol. 33, no. 8, pp. 1006-1011.